Russell Berrie Nanotechnology Institute
Technion - Israel Institute of Technology

Grand Technion Energy Program
Securing Israel today.
Transforming Israel's tomorrow.

Technion
Israel Institute of Technology

Schulich Faculty of Chemistry

The fundamental factors that determine the magneto-optical properties of colloidal quantum dots

Efrat Lifshitz, Schulich Faculty of Chemistry, Russell Berrie Nanotechnology Insitute and Solid State Institute, Technion, Israel

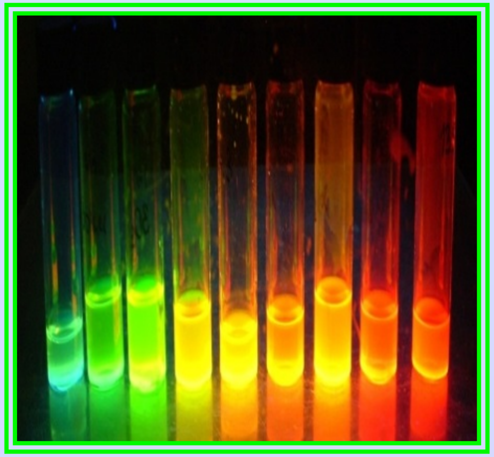

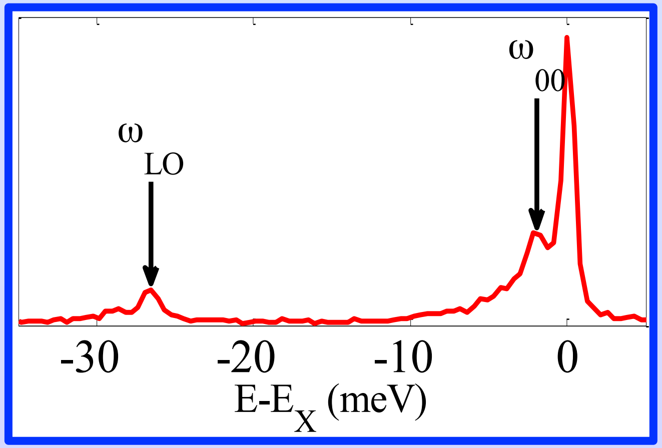

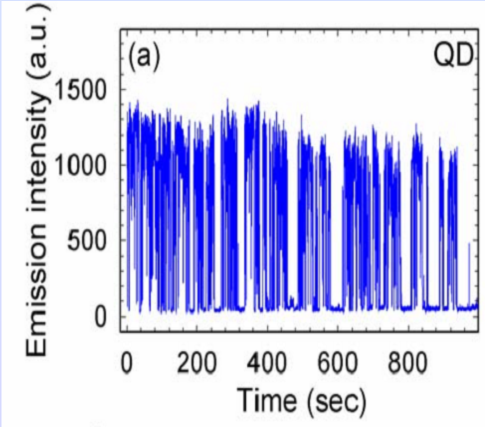

Semiconductor Nano-Structures

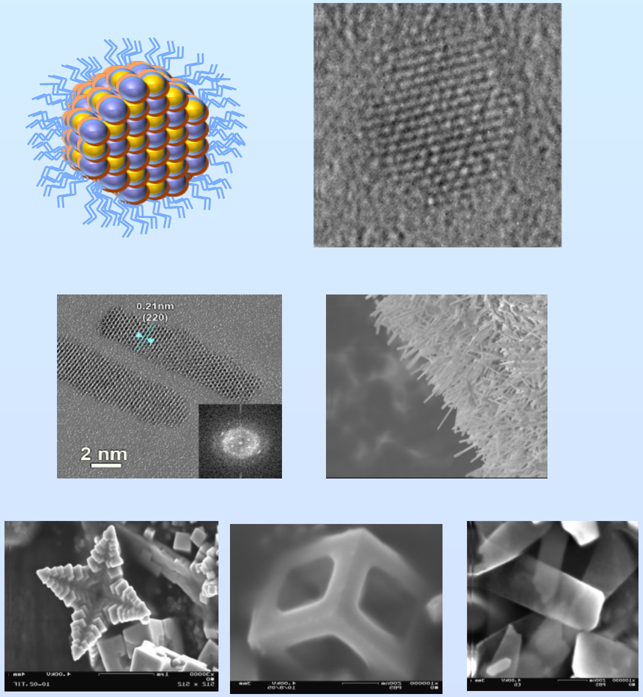

Zero- and One-dimensional:
Quantum dots (*top*), rods and wires (*middle*) and other shapes (*bottom*)

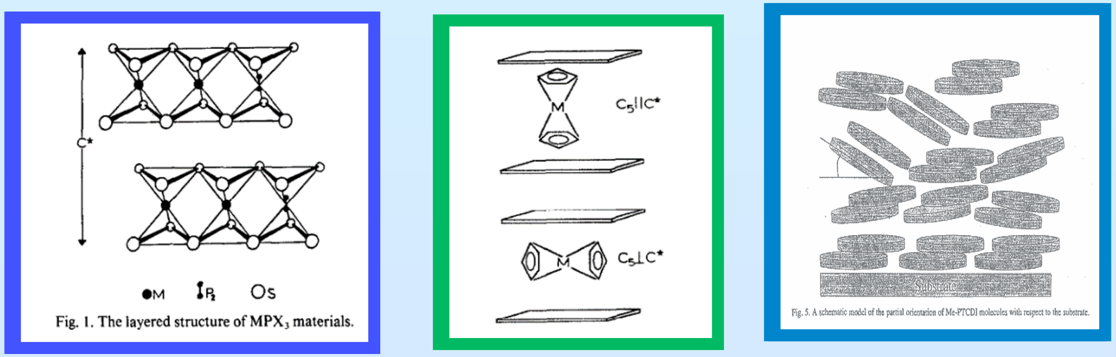

Two-dimensional: *Left to right*: Layered semiconductors, intercalation compounds and organic platelets

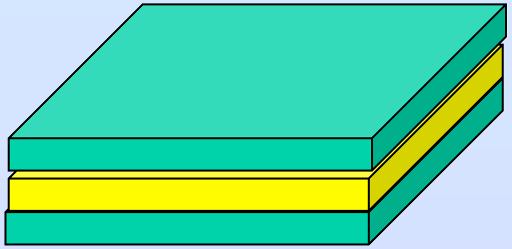

Two-dimensional :

Multiple quantum wells

Characterizing electronic states, and identifying carriers' trapping sites and their influence on: optical transitions and charge transport properties

Methods: Contactless magneto-optical methodologies

Optically detected magnetic resonance

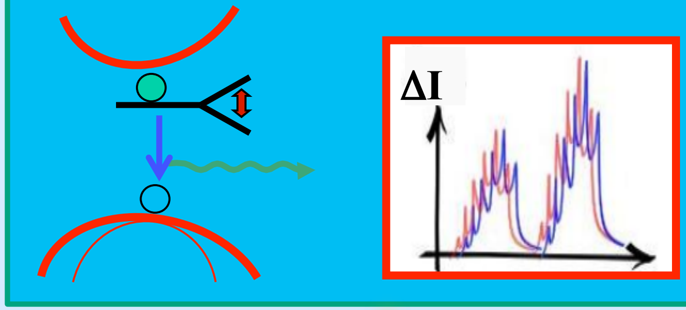

Circularly polarized Photoluminescence

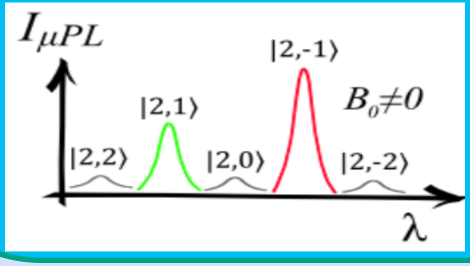

Magneto-Optical Spectroscopy

Optically detected cyclotron resonance

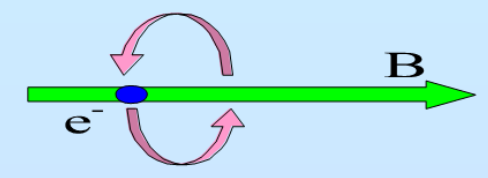

Micro-photoluminescence & AFM

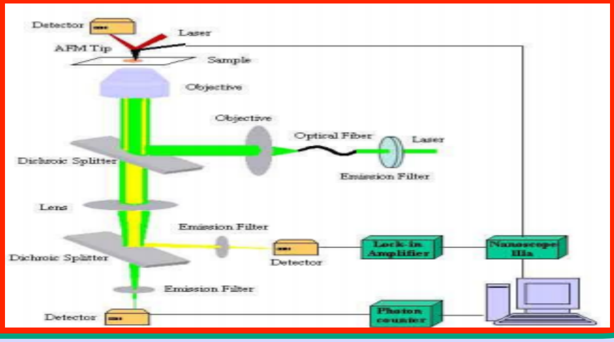

Micro-photoluminescence –single particle

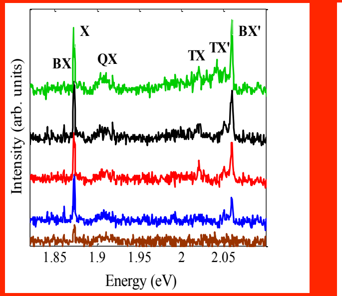

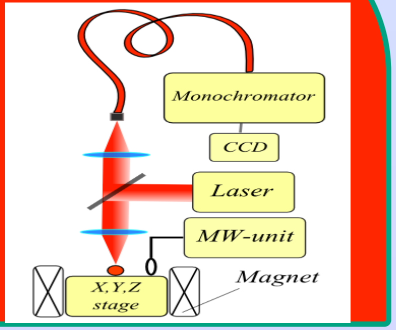

Quantum Dots (QDs)

stain growth

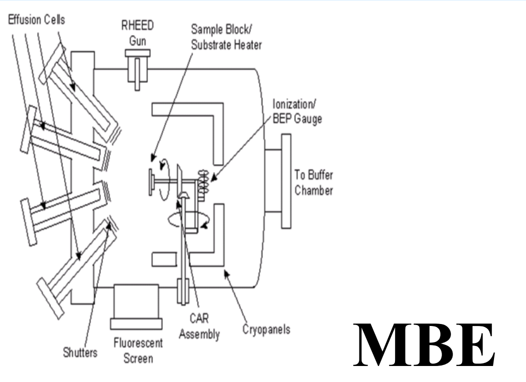

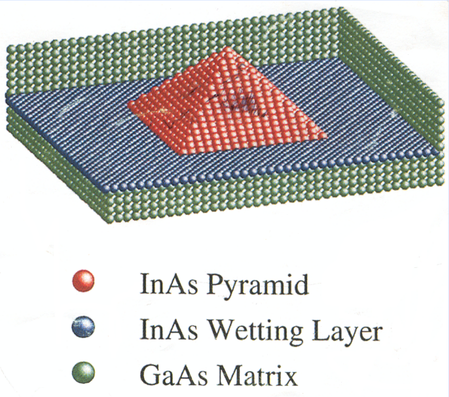

colloidal

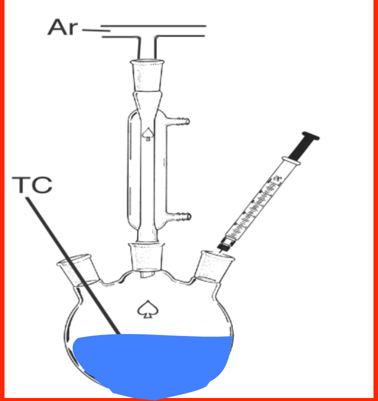

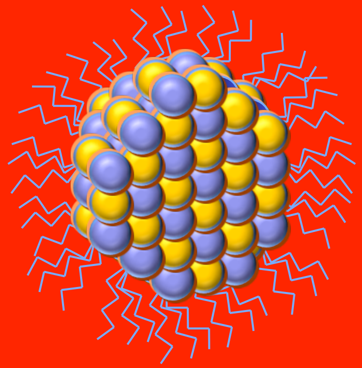

Free standing

spray

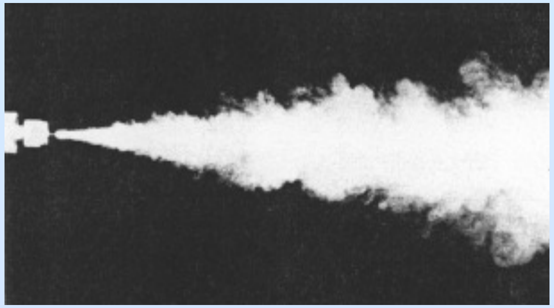

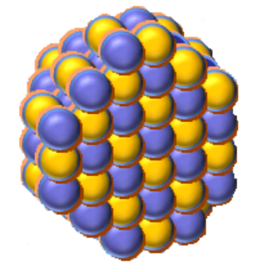

Physical method

Wet Chemistry methods

Nanocyrstals quantum dots (NQDs) active in the near infra-red

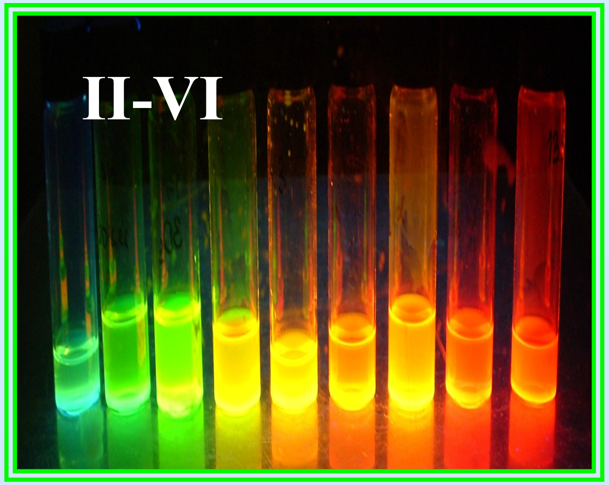

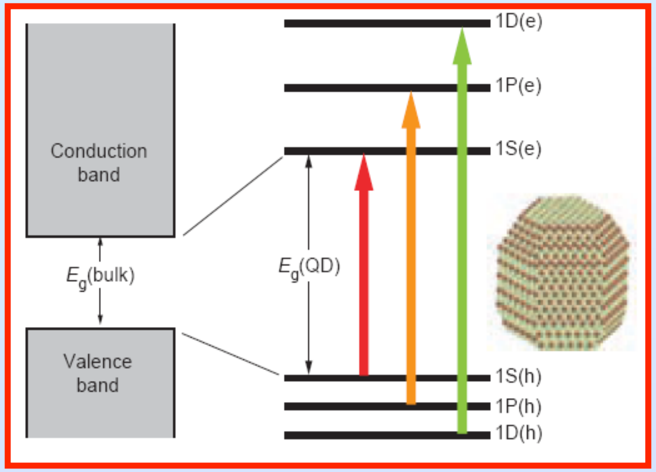

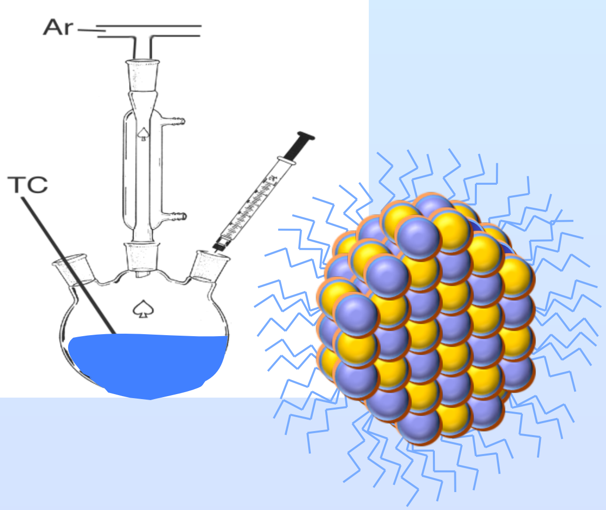

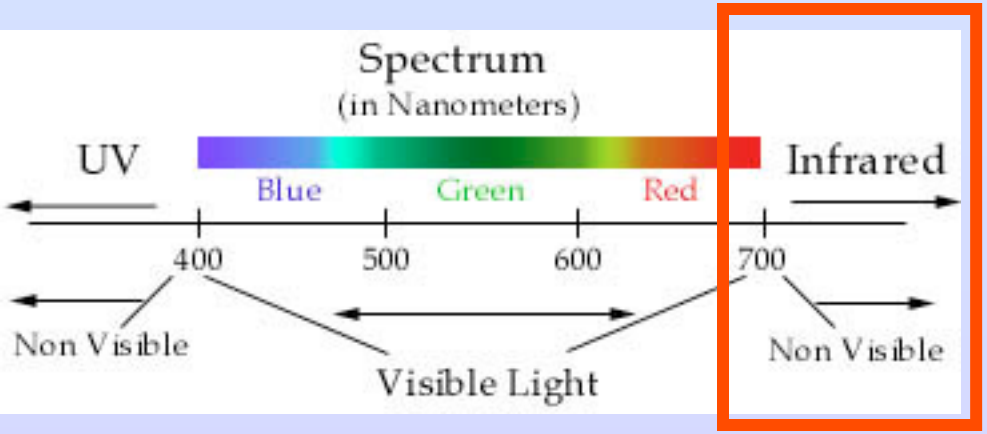

Applications:

PVs, LED, Photonics

Optical Switches,

Biological Platform

Spintronics

Applications: Photovoltiac, Gain device, optical switch

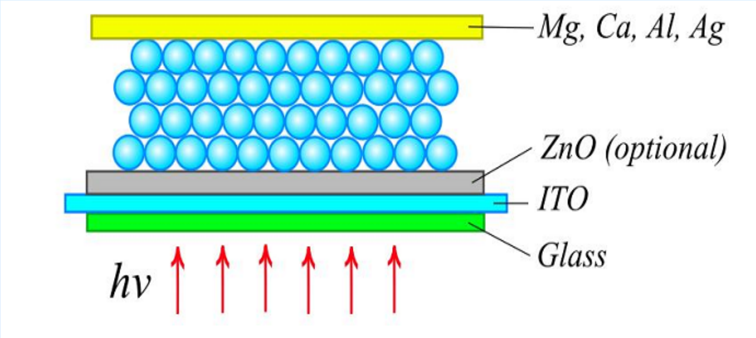

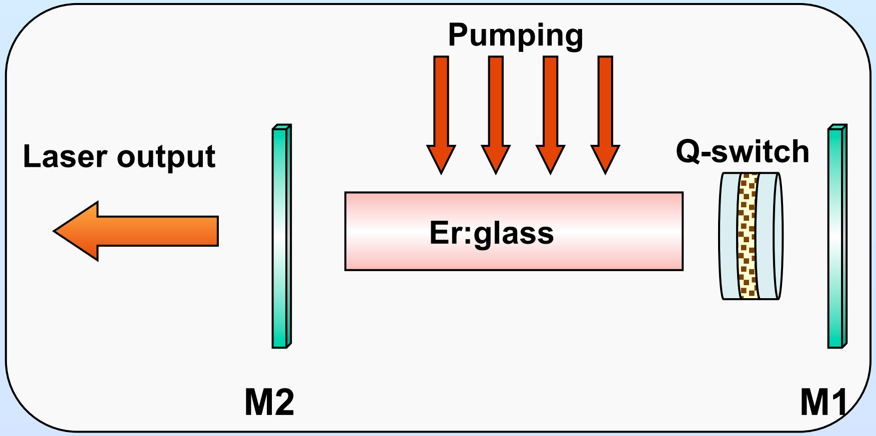

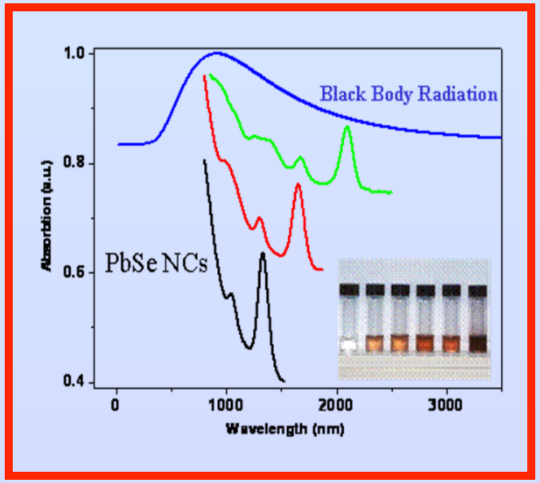

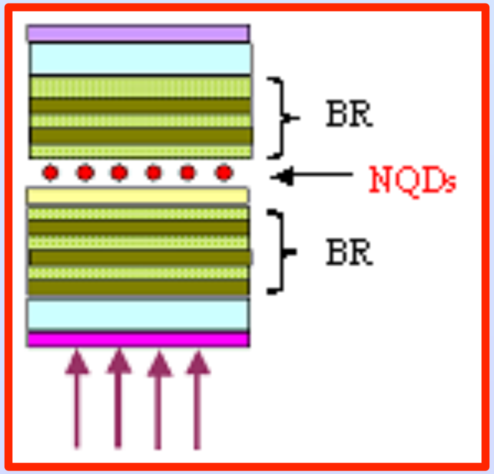

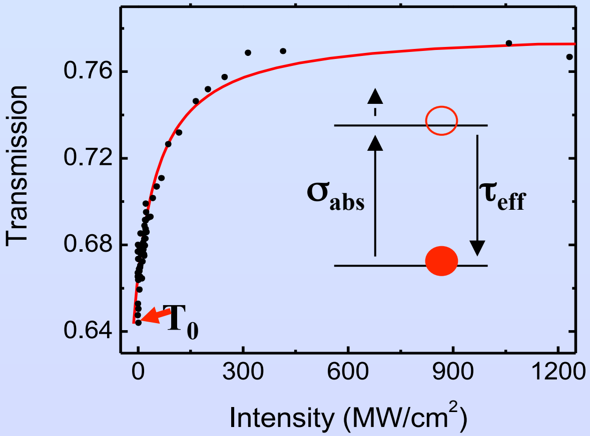

Content: What are the fundamental properties that control the magneto-optical properties of nanocrystals

- Internal or/and external properties (inorganic/organic omponents
- The strong/medium/weak confinement regimes
- Electronic band structure of core & core/shell nanocrystals
- Single and multiple-exciton
- Exchange interactions
- Hot carrier cooling
- Auger process and a way to mitigate it

Single dot measurements reveal knowledge about the fundamental points mentioned above

The role of ligands in colloidal quantum dots

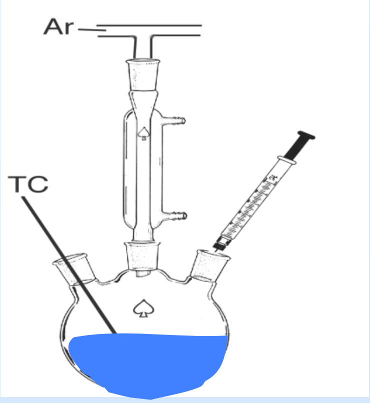

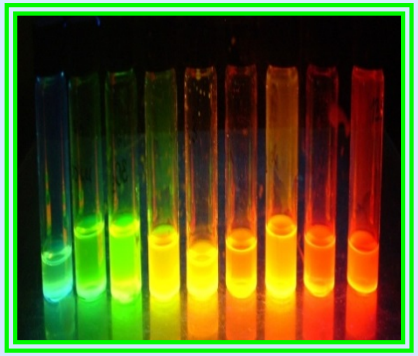

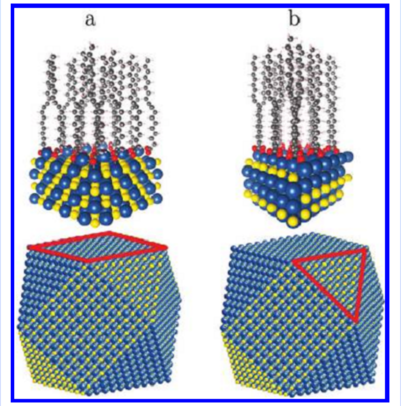

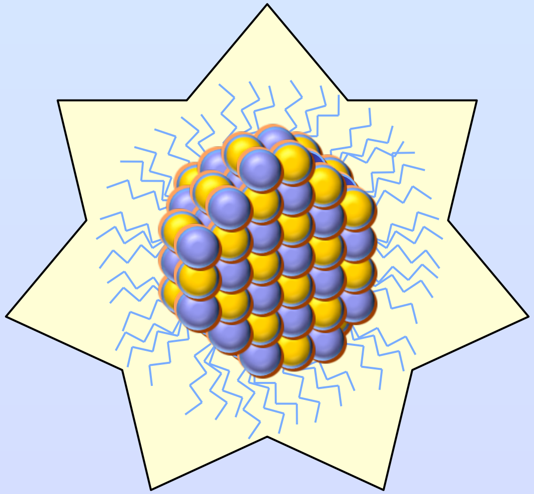

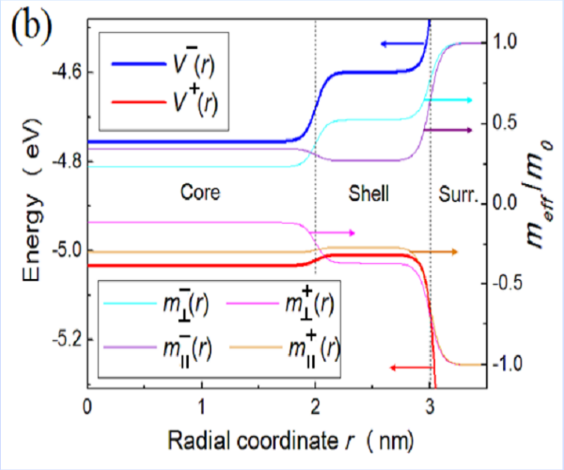

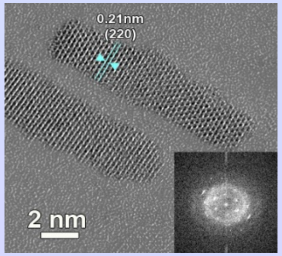

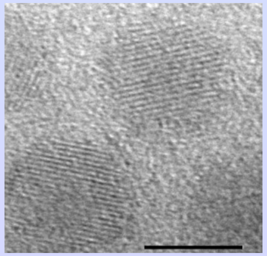

Ligands’ effect on hot carriers’ cooling and transport properties

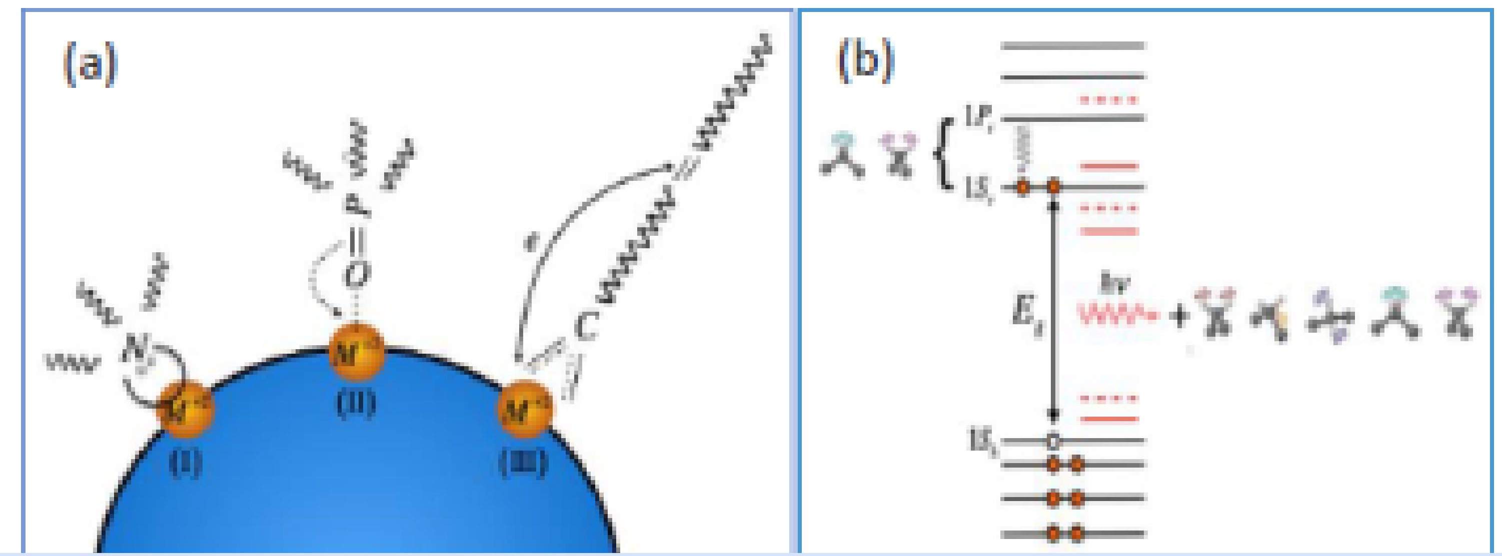

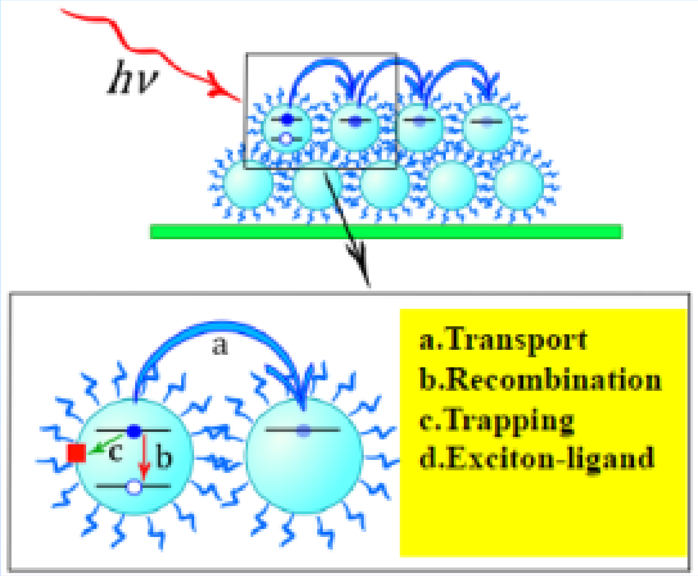

$$H = -\frac{\hbar^2}{2m_e}\nabla_e^2 - \frac{\hbar^2}{2m_h}\nabla_h^2 - \frac{e^2}{\varepsilon\left|\mathbf{r}_e - \mathbf{r}_h\right|}$$

Confinement regimes

Strong confinement: $R \ll a_{ex}$

- Confinement energy is much larger than the Coulomb interaction
- Coulomb interaction is treated as a perturbation

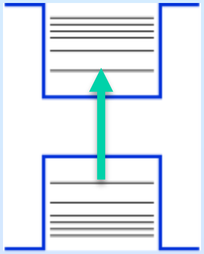

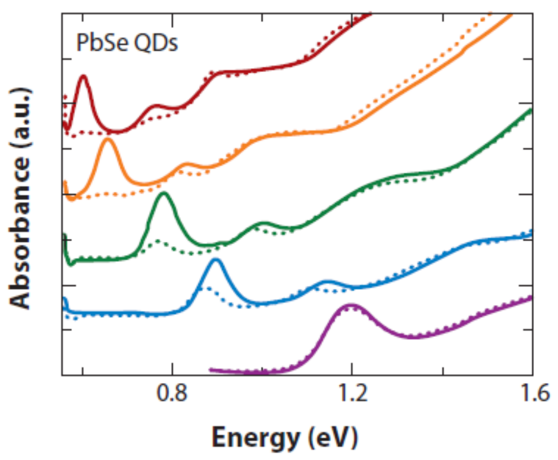

Annu. Rev. Condens. Mat. Phys. 5, 285 (2014)

Intermediate confinement: $R \sim a_{ex}$

- Confinement energy is comparable with the Coulomb interaction
- When $m_h \gg m_e$, hole moves in a mean potential created by strongly confined electron

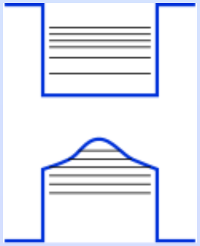

Weak confinement: $R \gg a_{ex}$

- The internal motion of the exciton is bulk-like (hydrogen-like spectrum)
- The exciton center-of-mass motion is confined within the nanocrystal

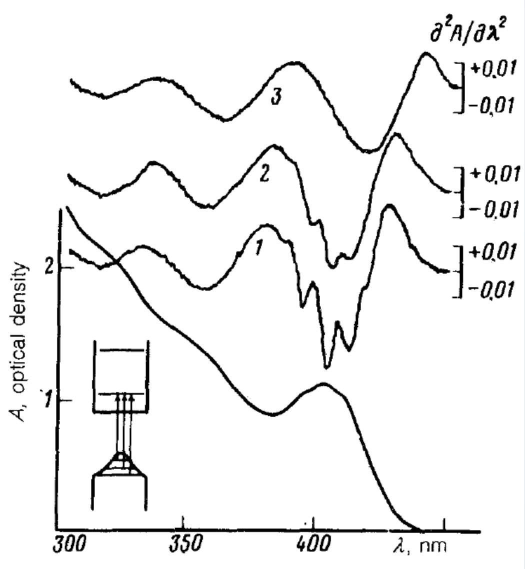

JETP Lett., 43, 376 (1986)

Excitonic fine structure

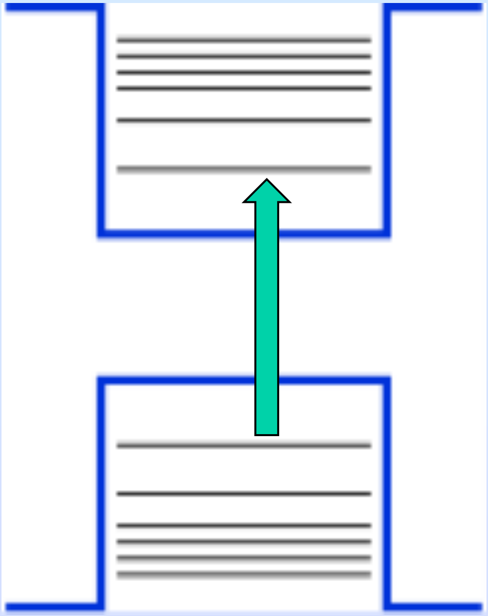

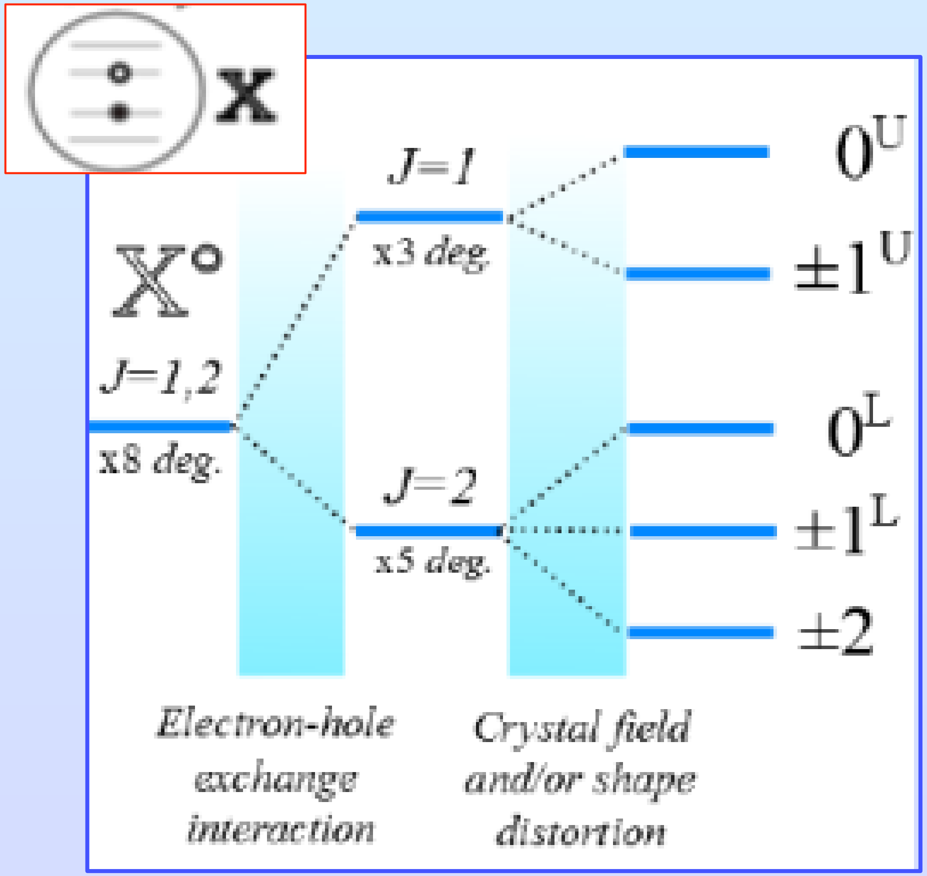

1Sh-1Se in II-VI semiconductors

Excitons

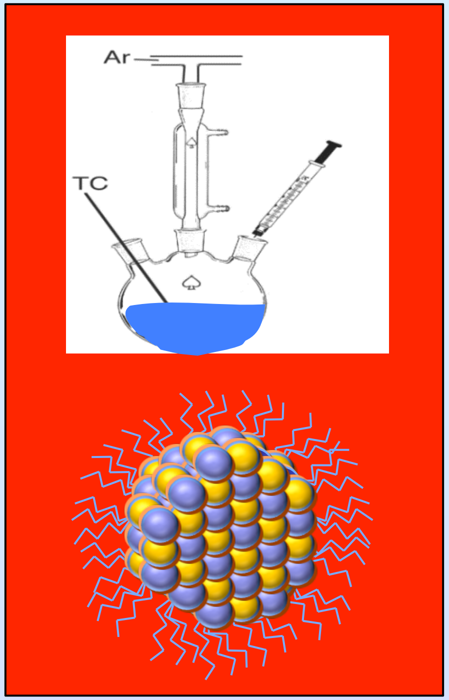

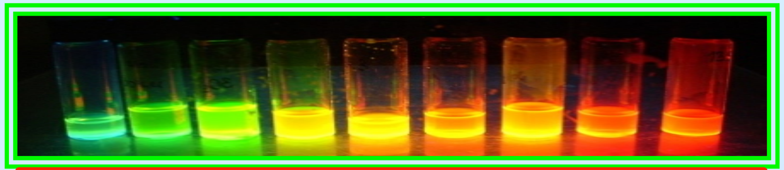

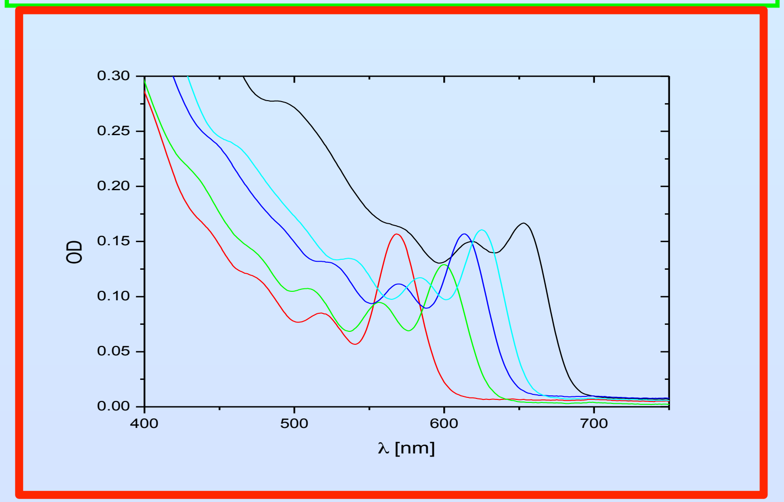

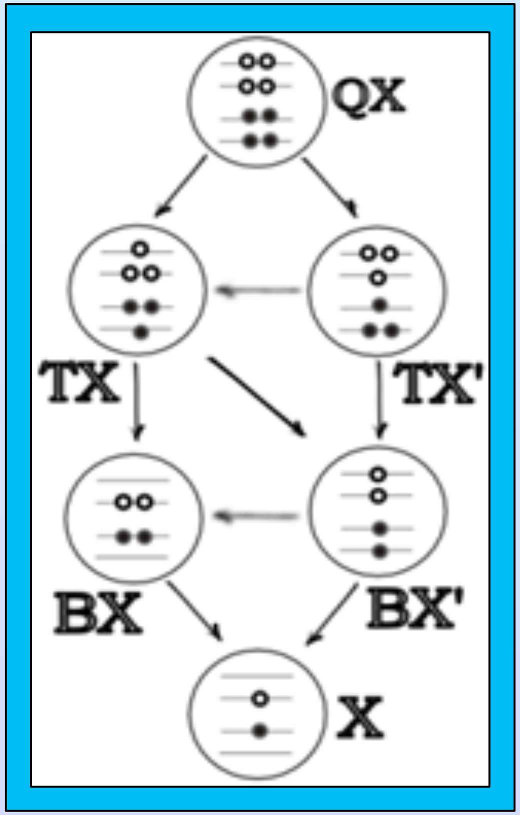

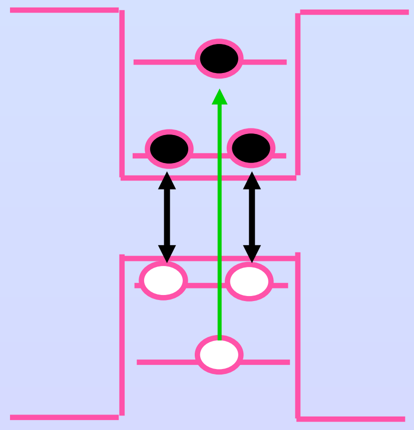

Sequential Filling

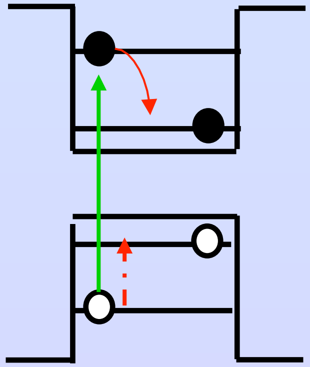

Multiple exciton generation

Blinking and spectral diffusion

Auger Process

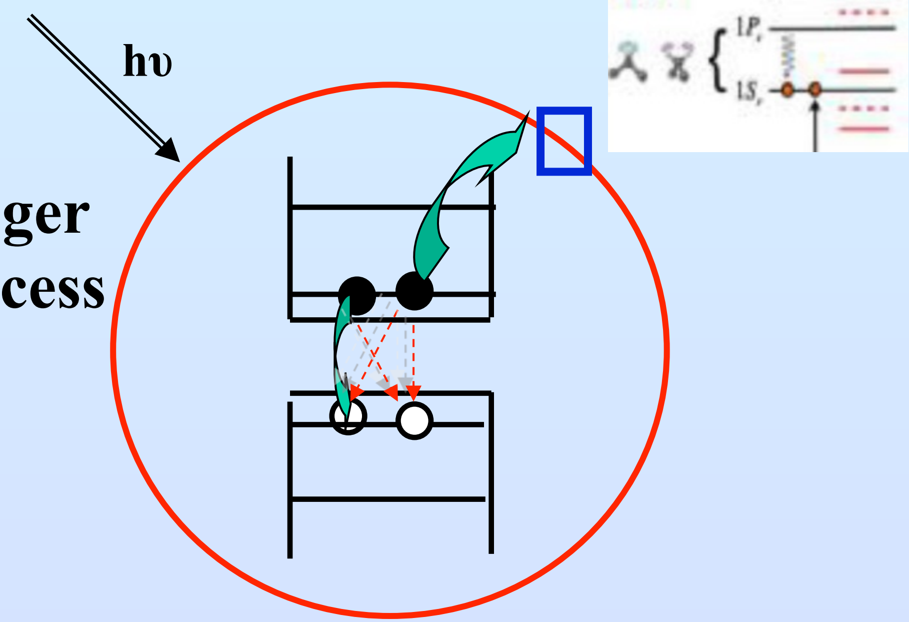

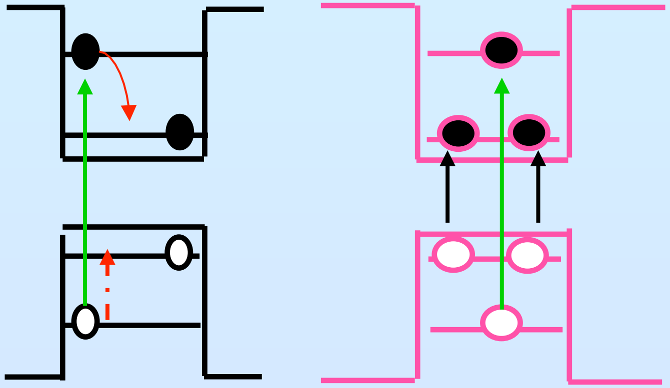

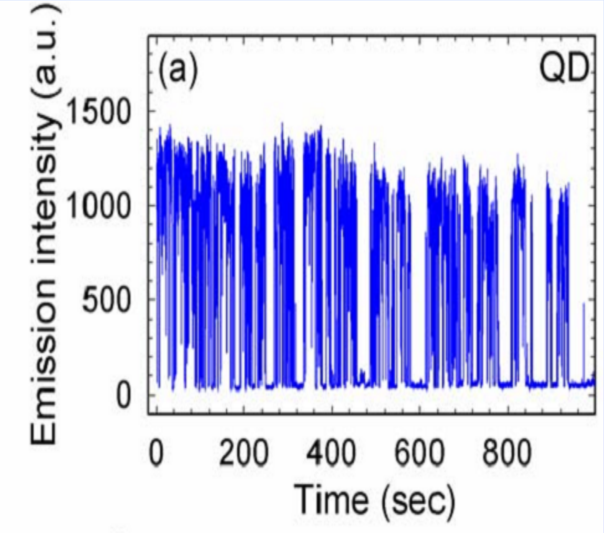

A. Efros/R. Marcus

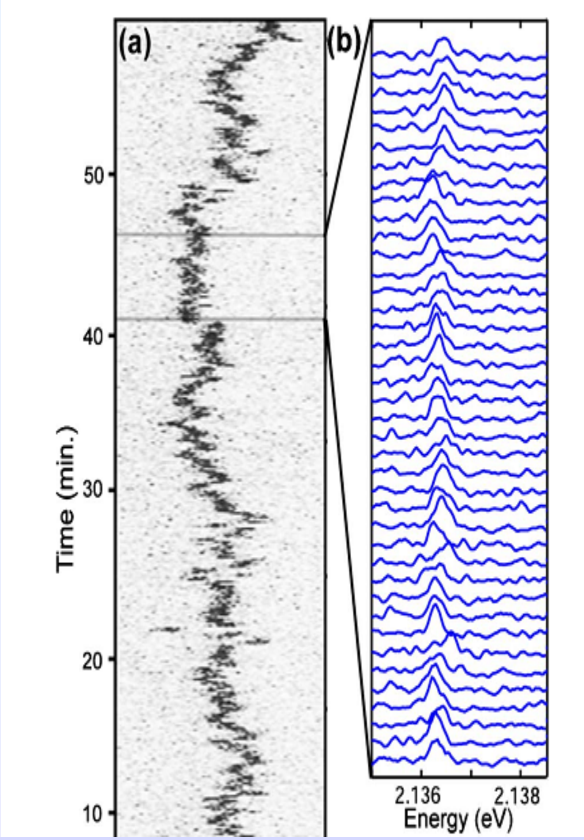

M. Fernee

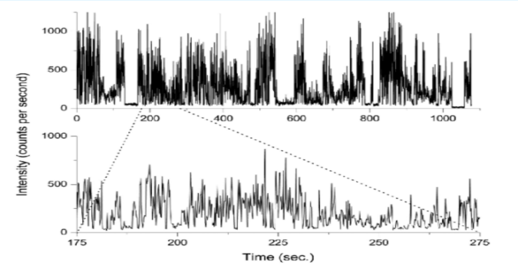

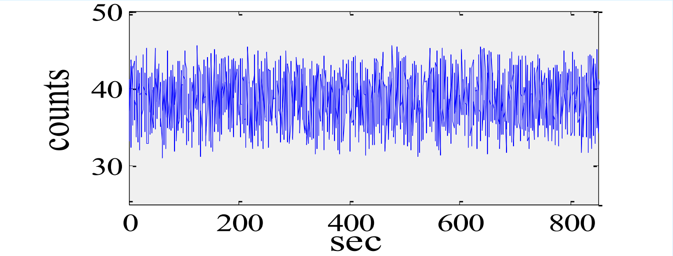

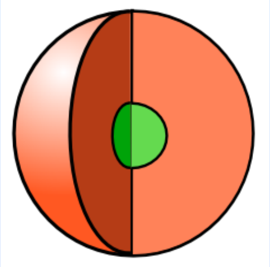

Giant-shell NC

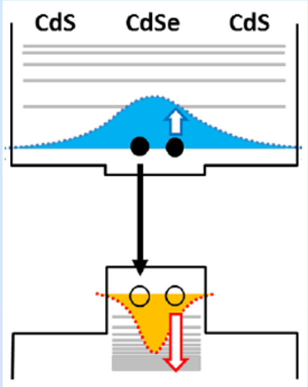

ACS Nano 7, 7288 (2014)

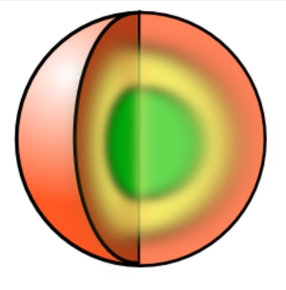

Alloyed core/shell NC

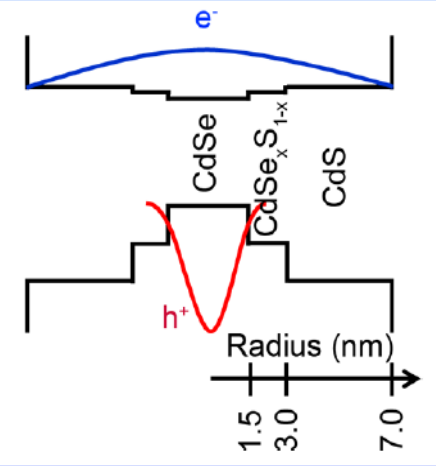

ACS Nano 7, 3411 (2013)

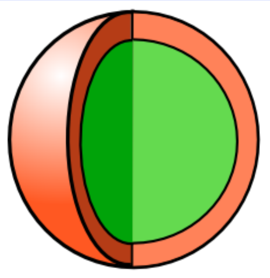

Giant-core NC

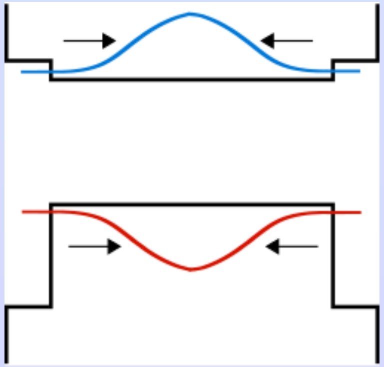

ODMR (PL-MR, or μPL-MR)

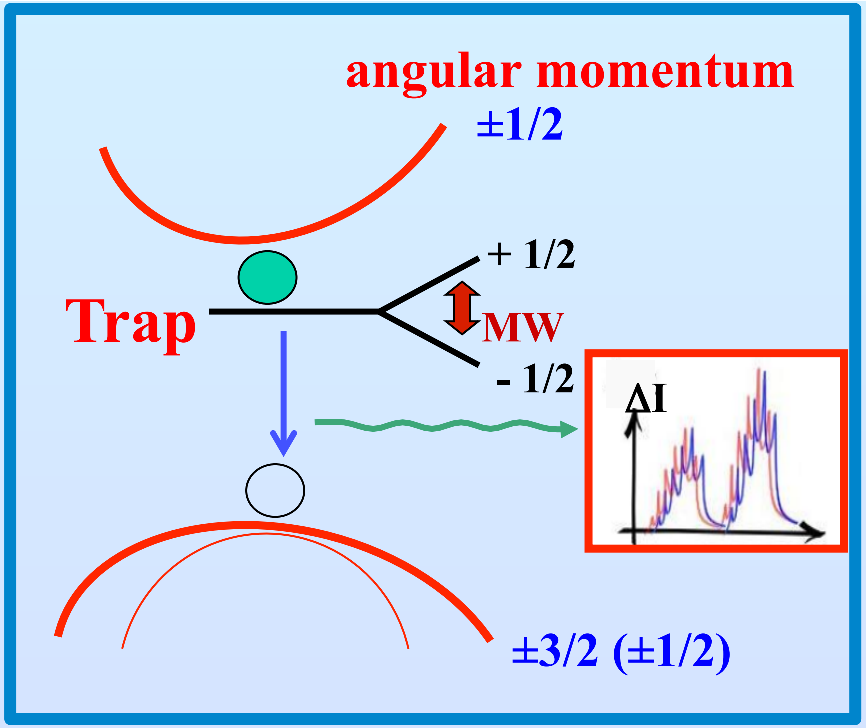
angular momentum

±1/2

Trap

+ 1/2

MW

- 1/2

ΔI

±3/2 (±1/2)

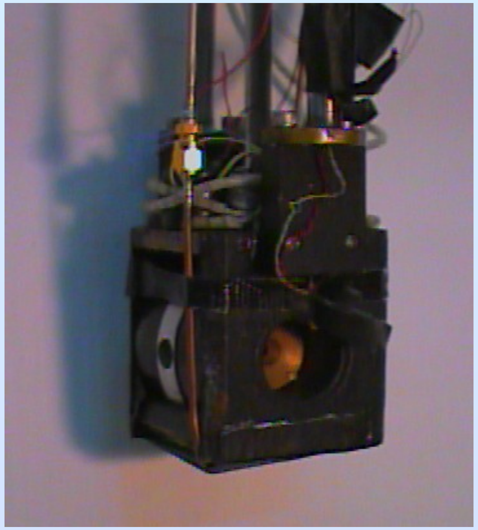

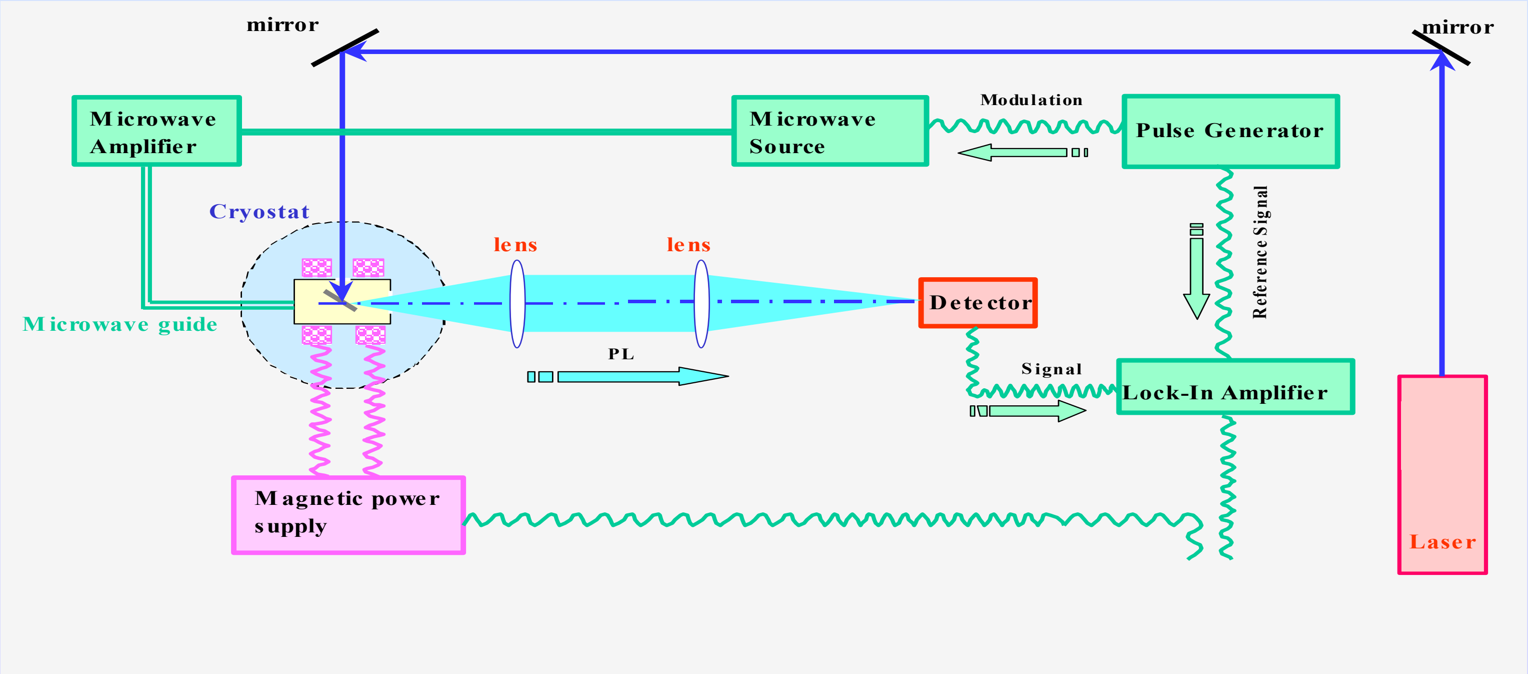
mirror

mirror

Microwave Amplifier

Microwave Source

Modulation

Pulse Generator

Cryostat

Reference Signal

lens

lens

Microwave guide

Detector

PL

Signal

Lock-In Amplifier

Magnetic power supply

Laser

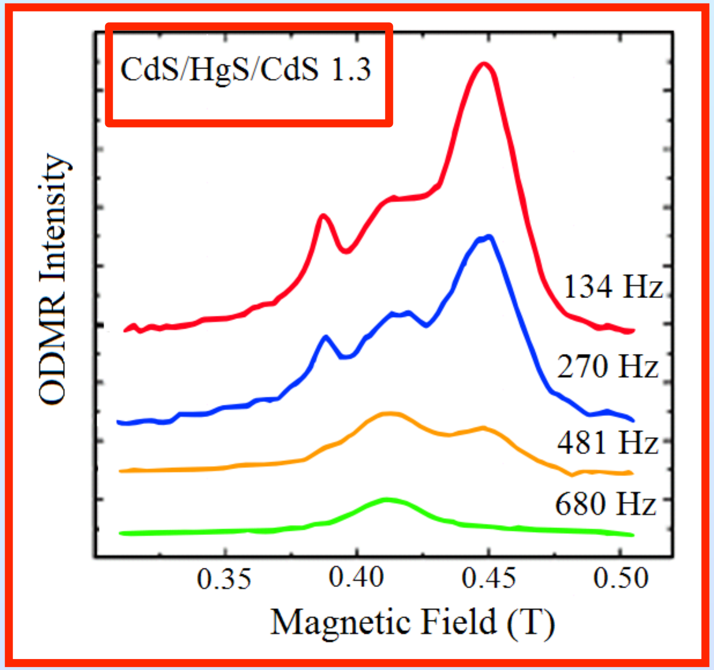
CdS/HgS/CdS 1.3
ODMR Intensity
134 Hz
270 Hz
481 Hz
680 Hz
0.35
0.40
0.45
0.50
Magnetic Field (T)

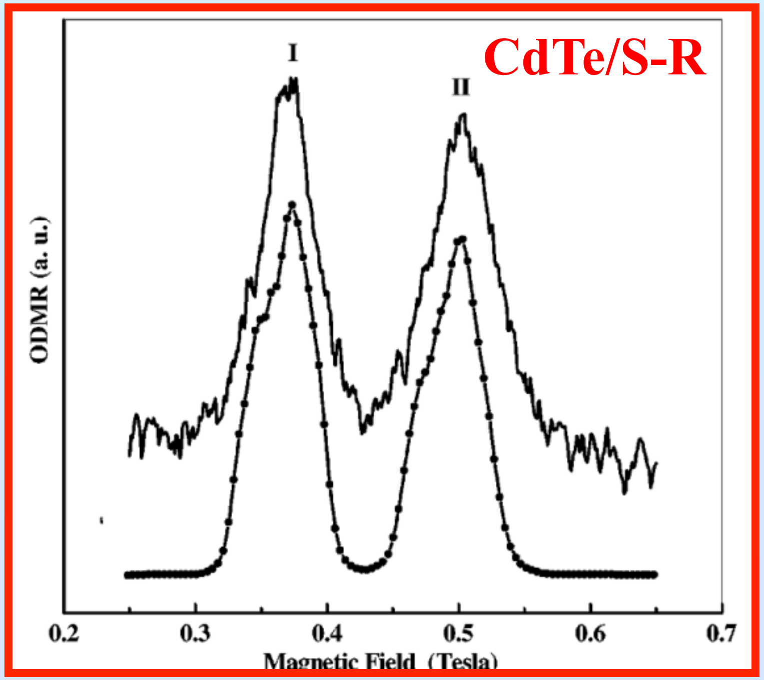
CdTe/S-R
I
II
ODMR (a. u.)
0.2
0.3
0.4
0.5
0.6
0.7
Magnetic Field (Tesla)

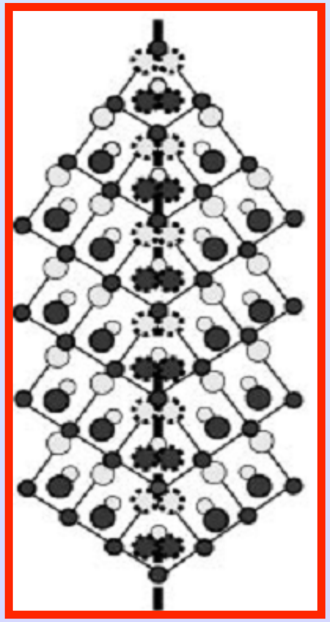

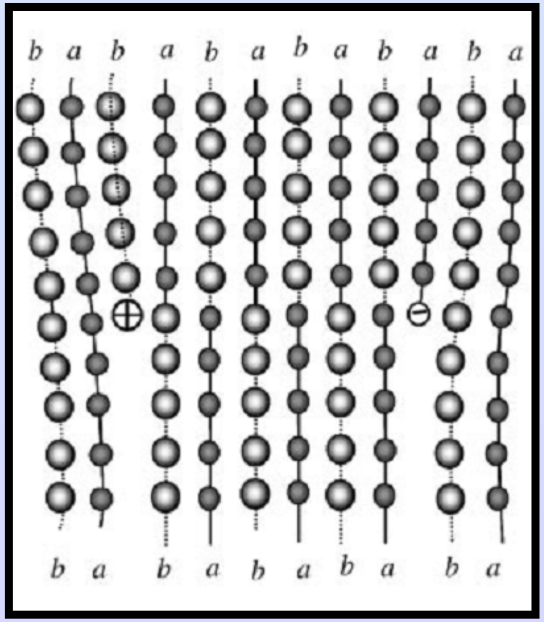
b a b a b a b a b a b a
b a b a b a b a b a

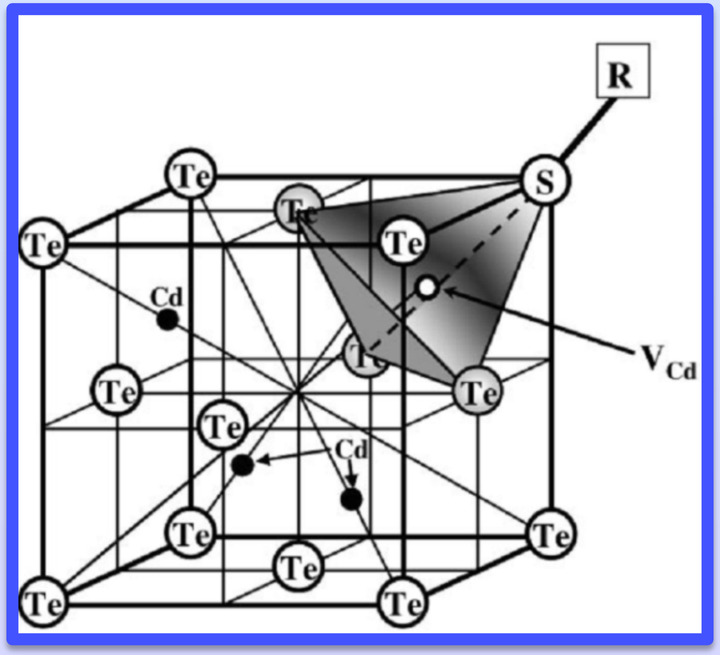
R
S
Te
Cd
Cd
V_{Cd}

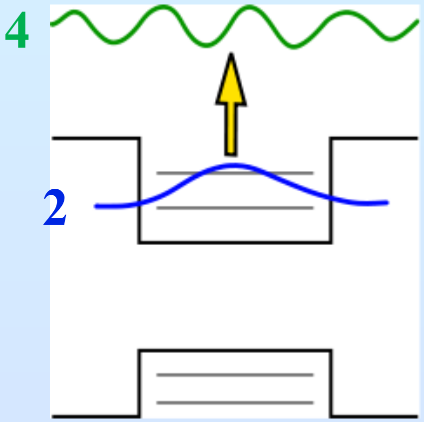

Electron

excitation

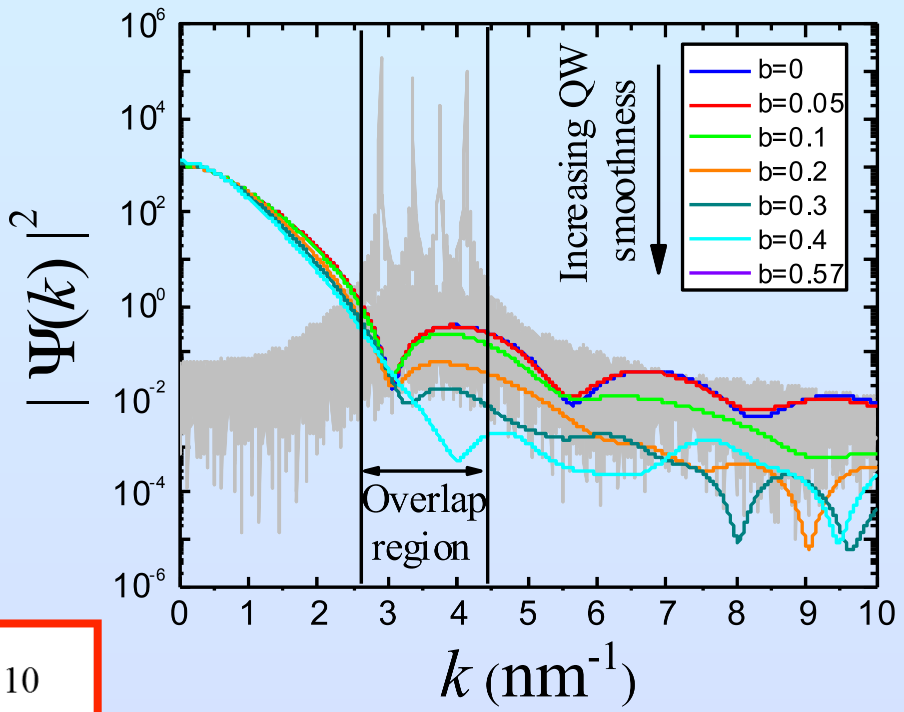

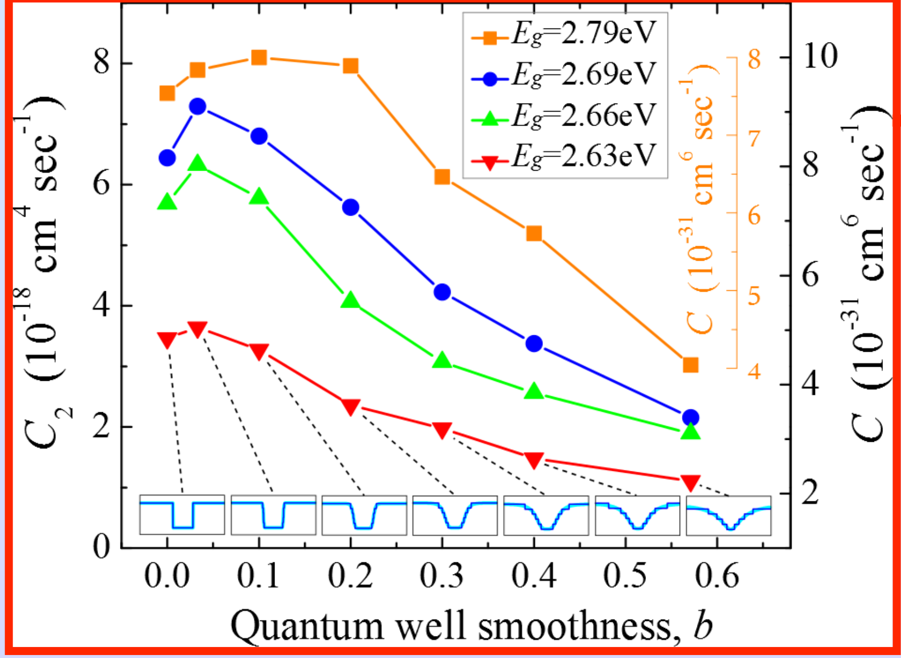

R. Vaxenburg, E. Lifshitz, A. Efros,

Appl. Phys. Lett., 2013 (1 & 2)

ELECTRONIC PROPERTIES OF QUANTUM DOTS WITH ALLOY COMPOSITION

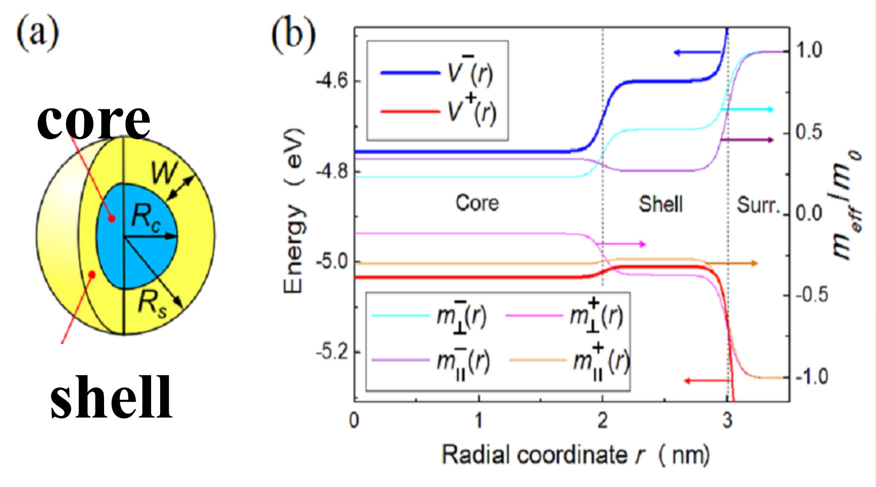

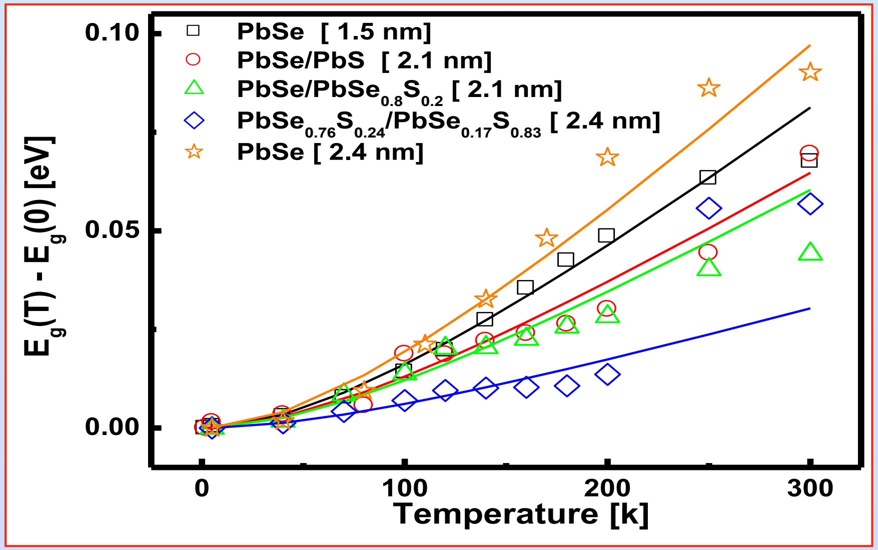

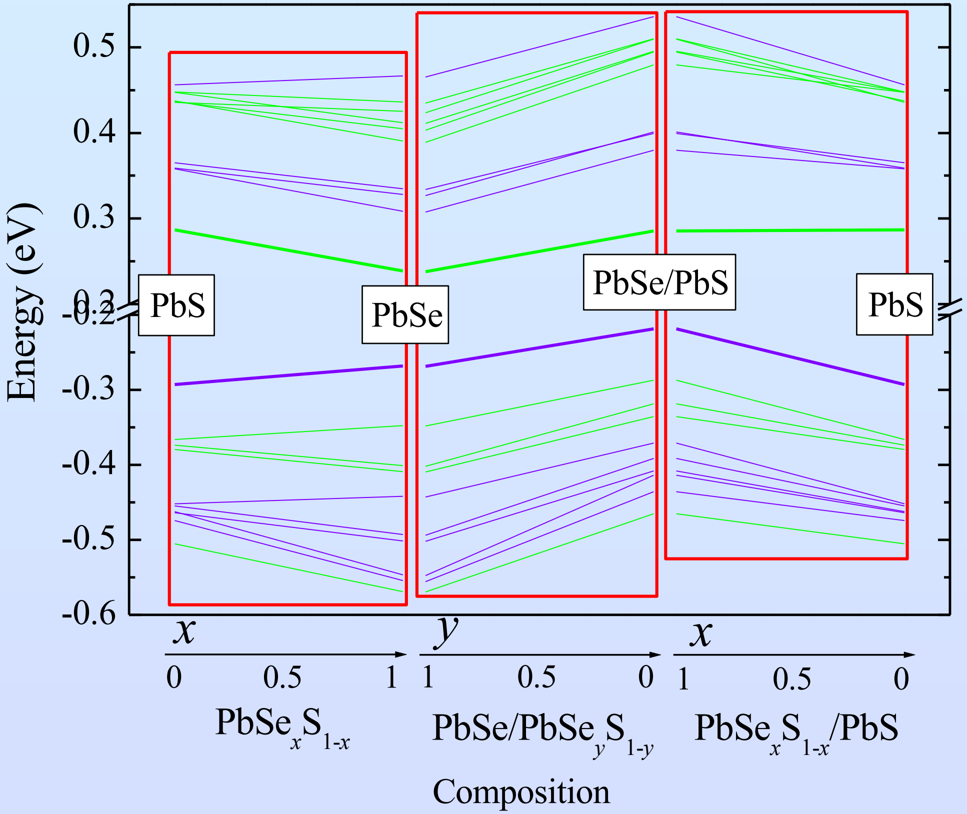

$$\lambda(r) = \lambda_A + (\lambda_B - \lambda_A)\Theta(r - R_c) + (\lambda_C - \lambda_B)\Theta(r - R_s)$$

$$\Theta(r) \equiv \frac{1}{2}\left(1 + \tanh(\gamma r)\right)$$

PRB, 2012, 85, 075304; ACSNano 2010, 4, 6547;Small 2009, 5, 1674;Nanoscale, Review, 2013

Experimental Evidences

R~2.5 nm

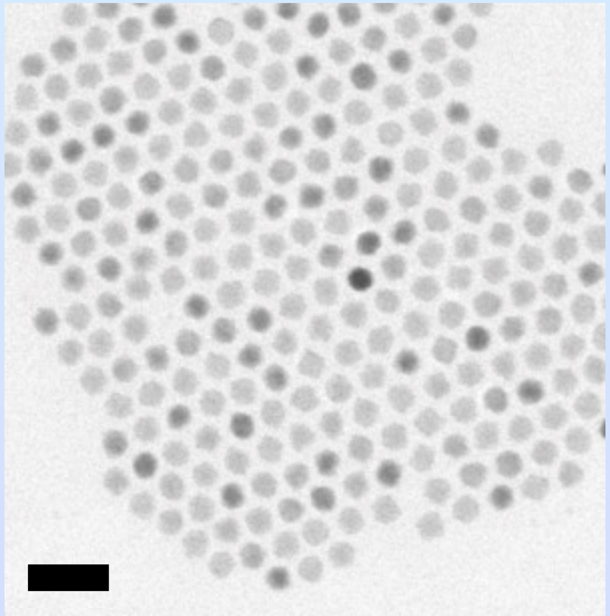

20 nm

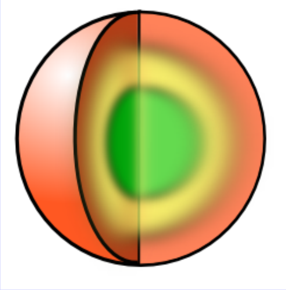

R~6.25 nm

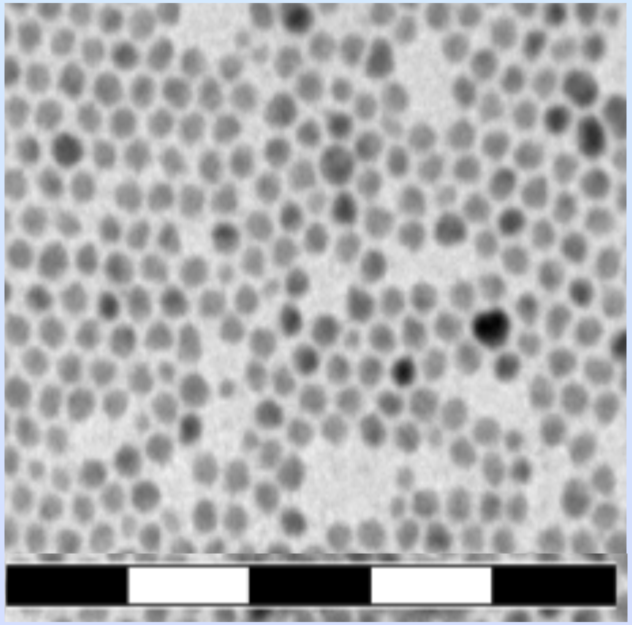

200 nm

R~12.5 nm

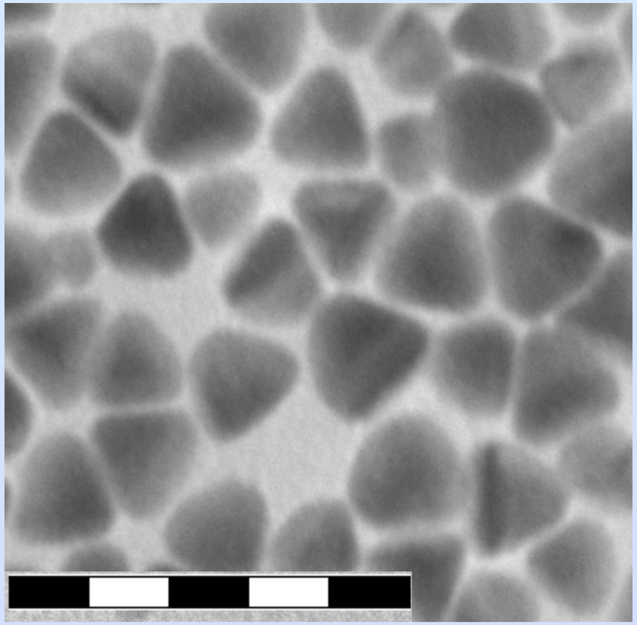

100 nm

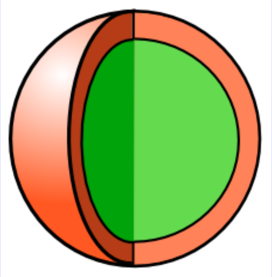

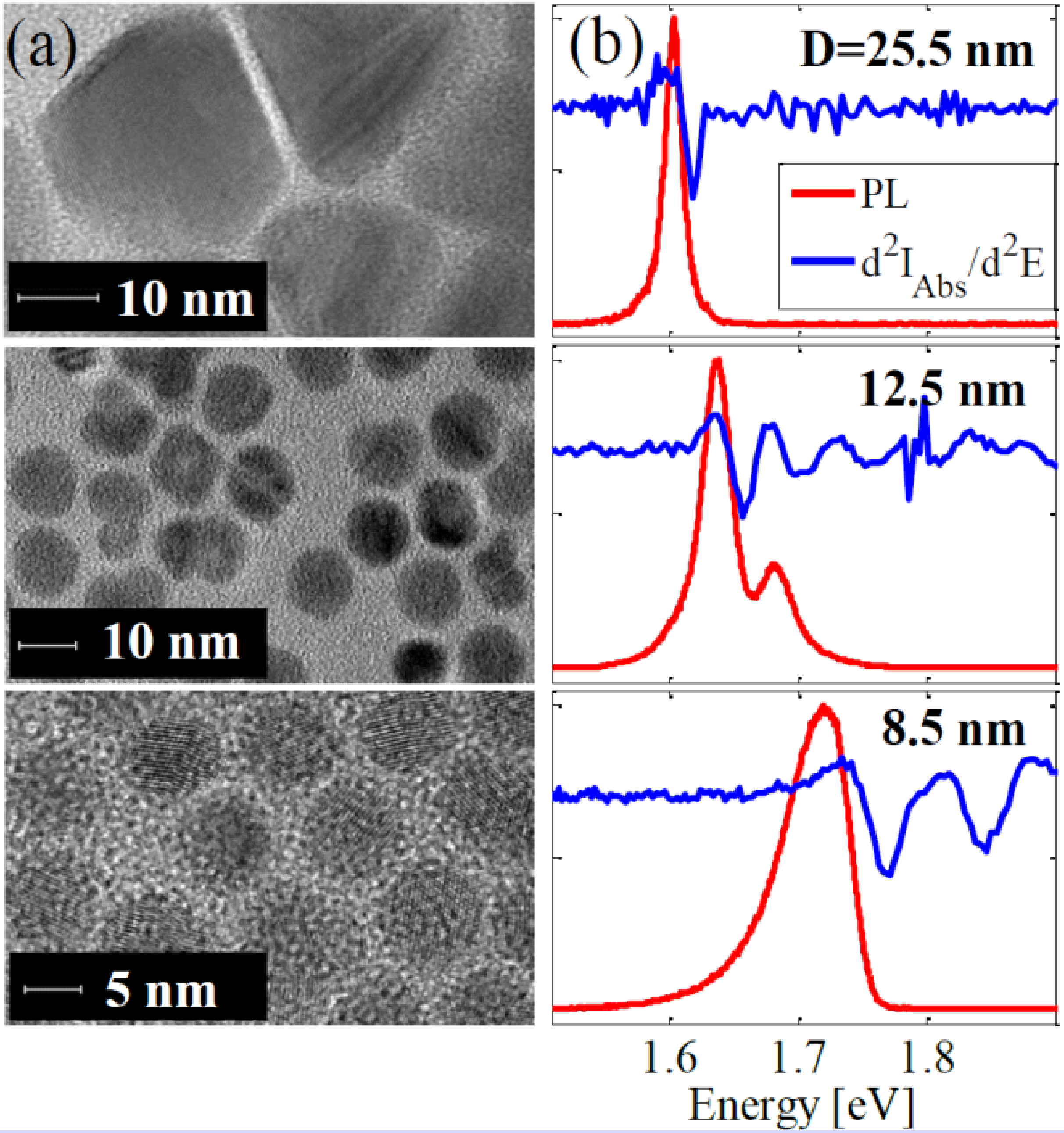
(a)
10 nm
10 nm
5 nm
(b)
D=25.5 nm
PL
d^2I_{Abs}/d^2E
12.5 nm
8.5 nm
1.6
1.7
1.8
Energy [eV]

Direct view of magneto-optical properties by a single dot spectroscopy

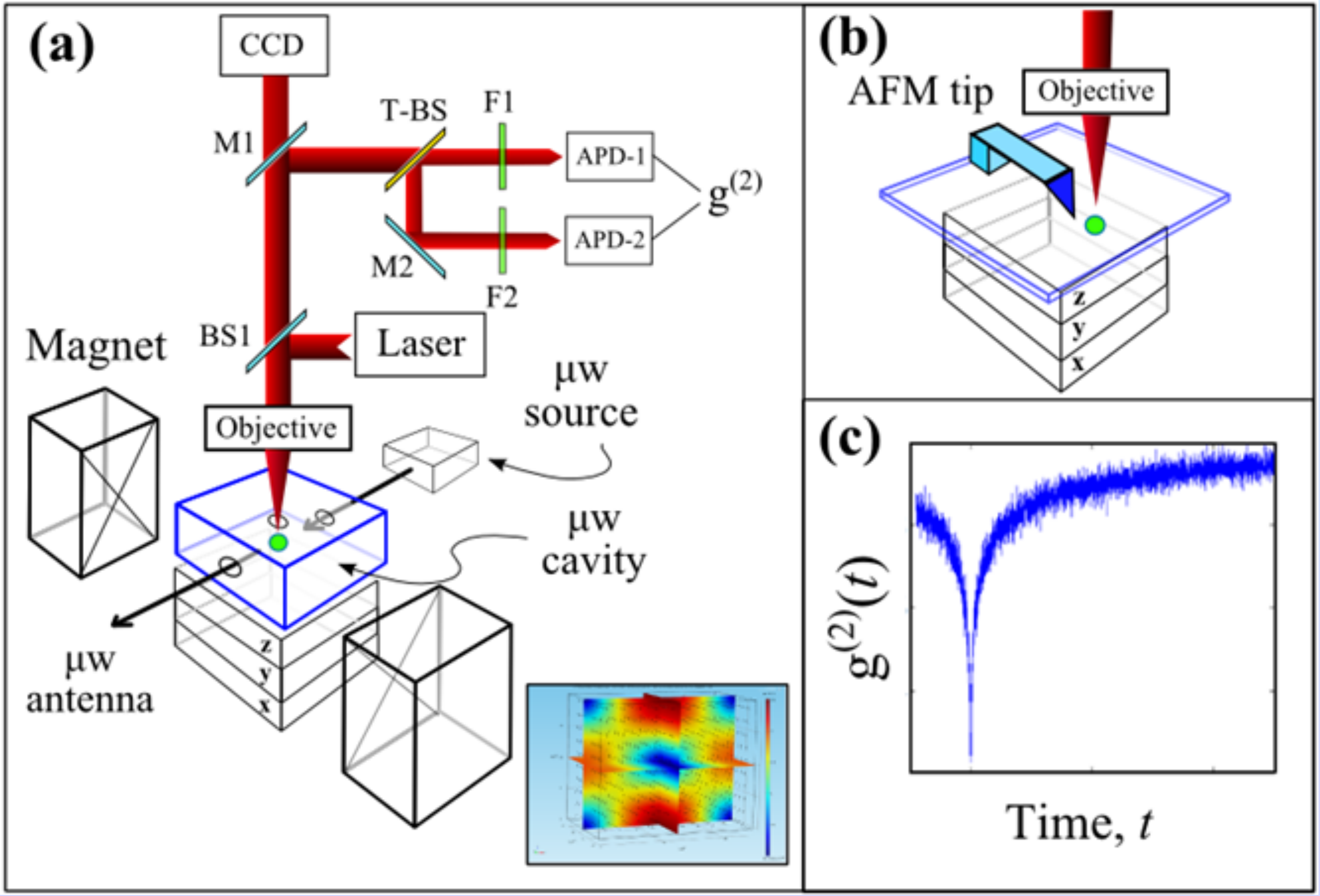

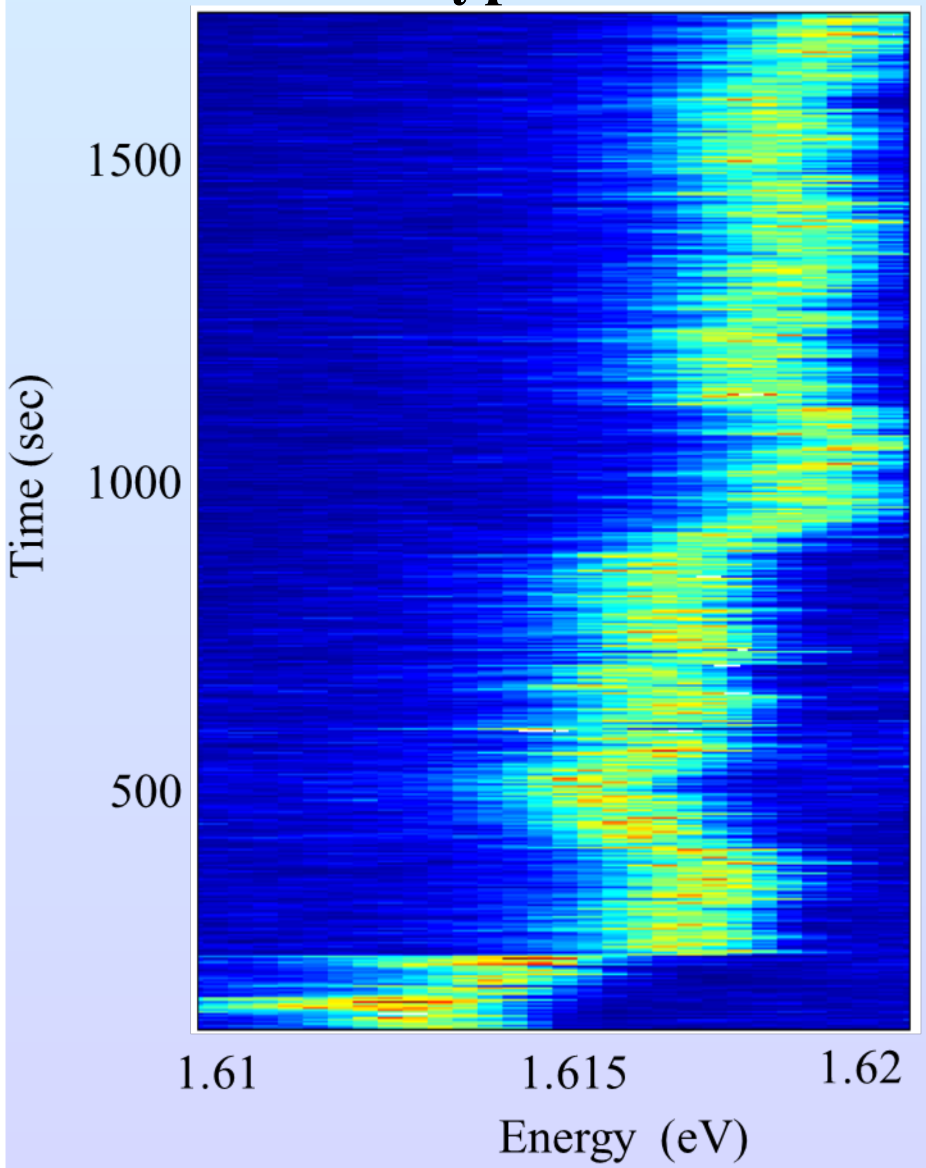

Typical 2.75 eV

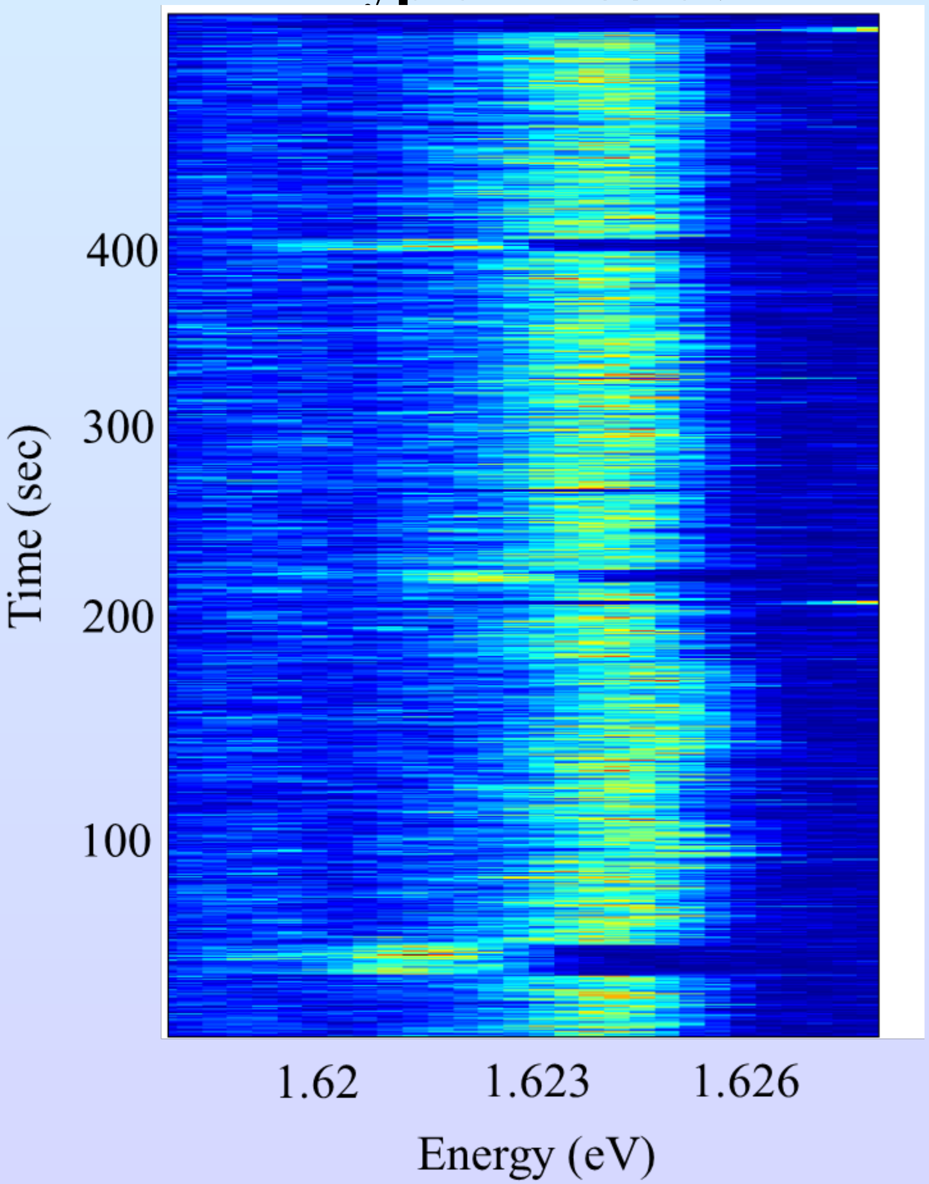

Typical 1.87 eV

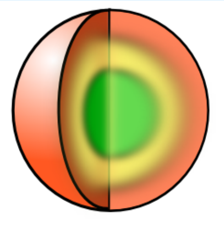

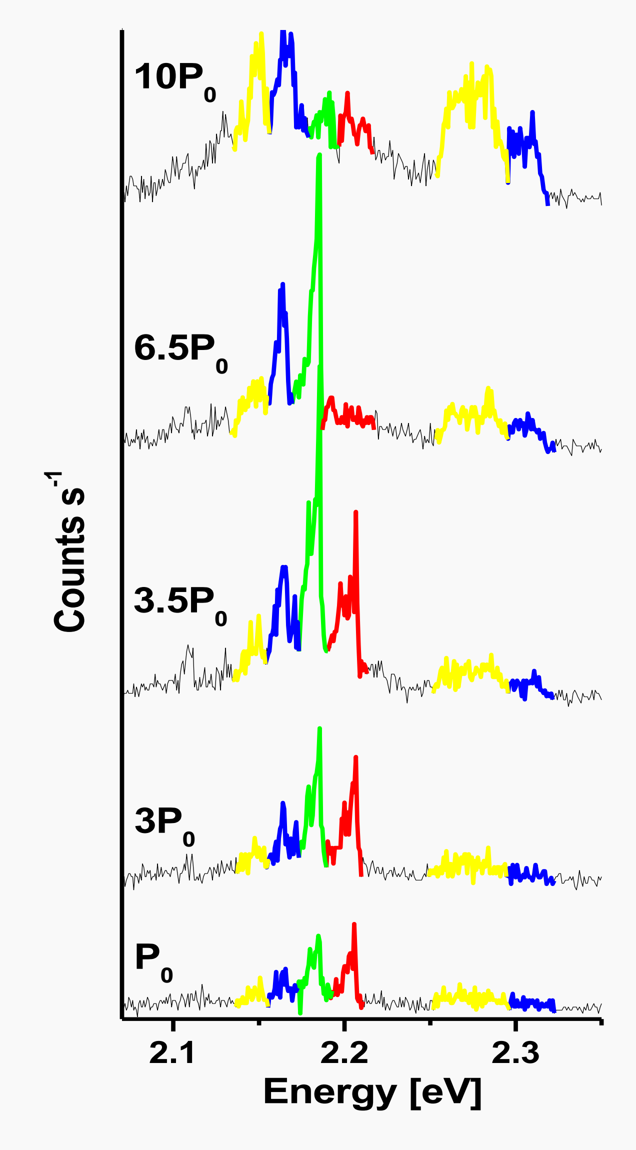

$$< N >= P_{exc}\sigma j_p$$

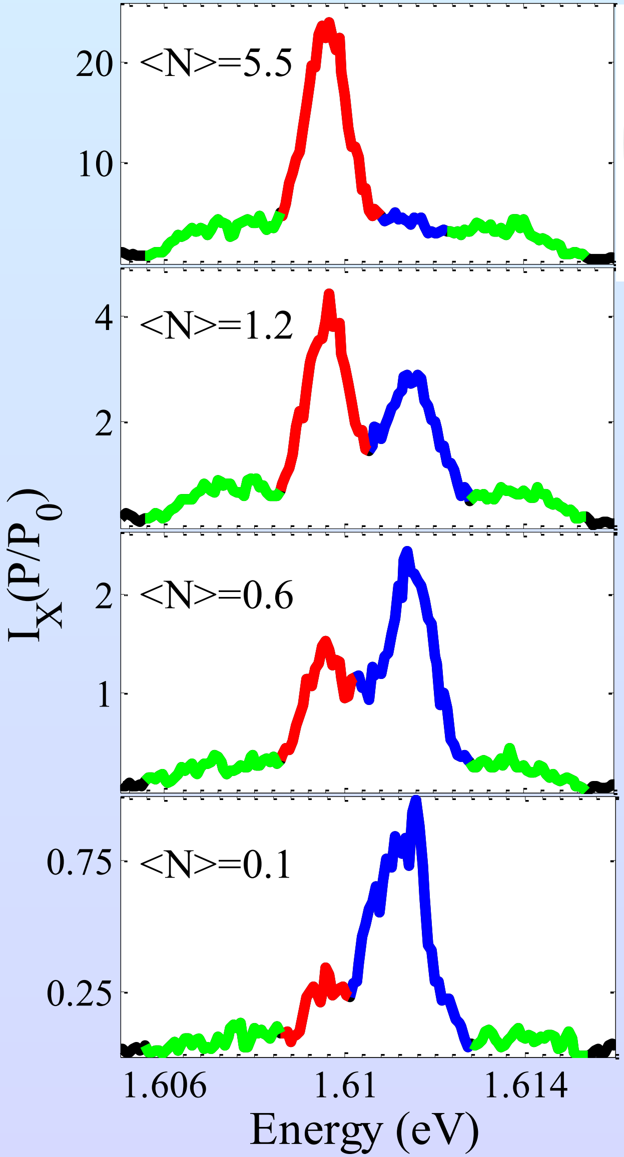

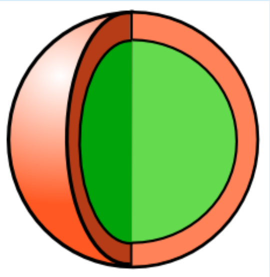

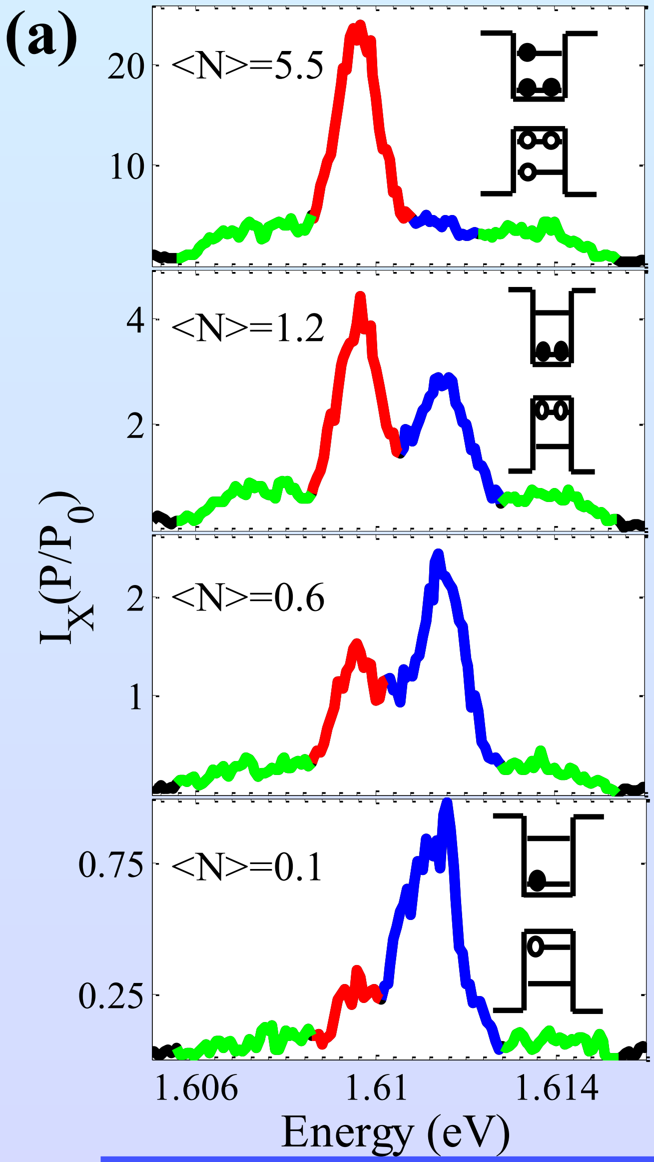

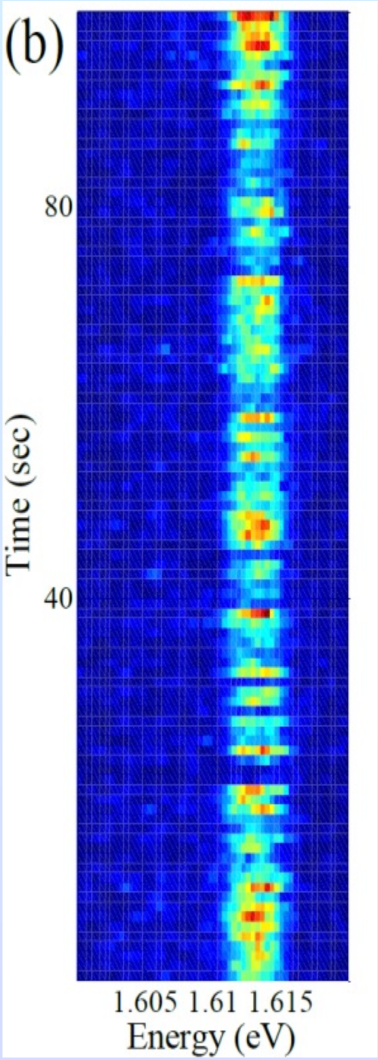

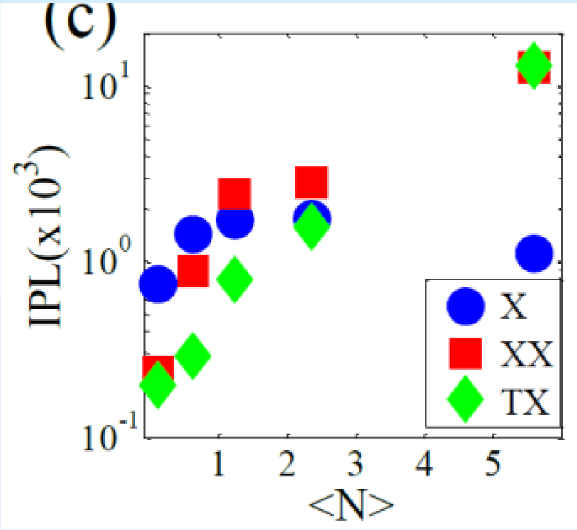

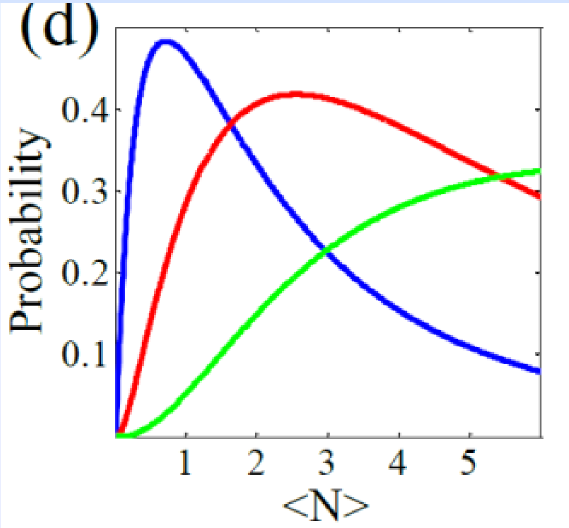

$$\mathbf{V_c}\left(\mathbf{r}_{1,e},\mathbf{r}_{2,e}..\mathbf{r}_{n,e},\mathbf{r}_{1,h},\mathbf{r}_{2,h},..\mathbf{r}_{n,h}\right)=\sum_{i=1}^{n}\sum_{j=1}^{n}V_{int}\left(\left|\mathbf{r}_{i,e}-\mathbf{r}_{j,h}\right|\right)-\sum_{i\neq j=1}^{n}V_{int}\left(\left|\mathbf{r}_{i,e(h)}-\mathbf{r}_{j,e(h)}\right|\right)+\sum_{i=1}^{n}V_p\left(\mathbf{r}_{i,e}\right)+\sum_{i=1}^{n}V_p\left(\mathbf{r}_{i,h}\right)$$

Theory *vs.* Experiment

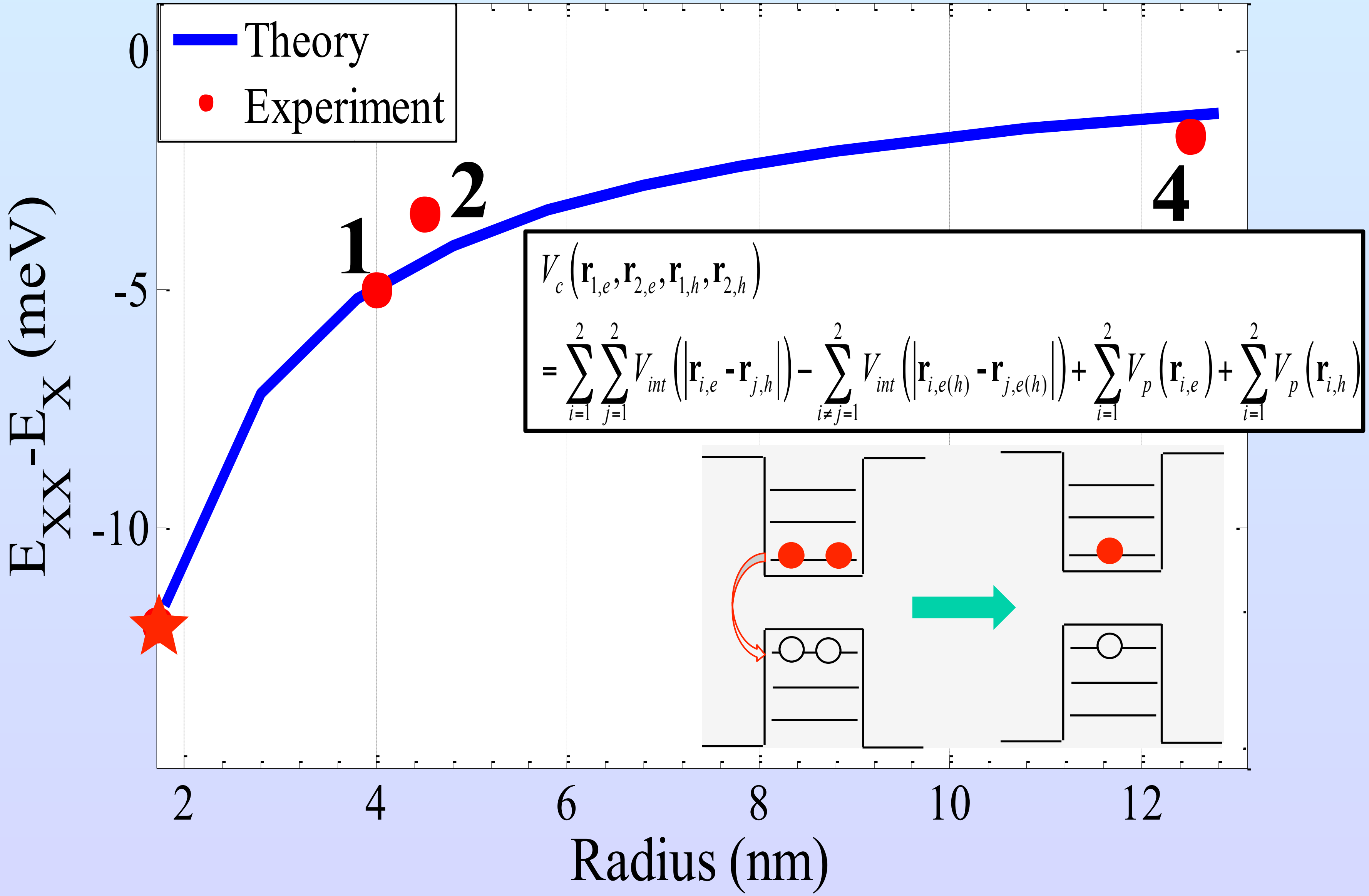

$$V_c\left(\mathbf{r}_{1,e},\mathbf{r}_{2,e},\mathbf{r}_{1,h},\mathbf{r}_{2,h}\right)$$

$$=\sum_{i=1}^{2}\sum_{j=1}^{2}V_{int}\left(\left|\mathbf{r}_{i,e}-\mathbf{r}_{j,h}\right|\right)-\sum_{i\neq j=1}^{2}V_{int}\left(\left|\mathbf{r}_{i,e(h)}-\mathbf{r}_{j,e(h)}\right|\right)+\sum_{i=1}^{2}V_p\left(\mathbf{r}_{i,e}\right)+\sum_{i=1}^{2}V_p\left(\mathbf{r}_{i,h}\right)$$

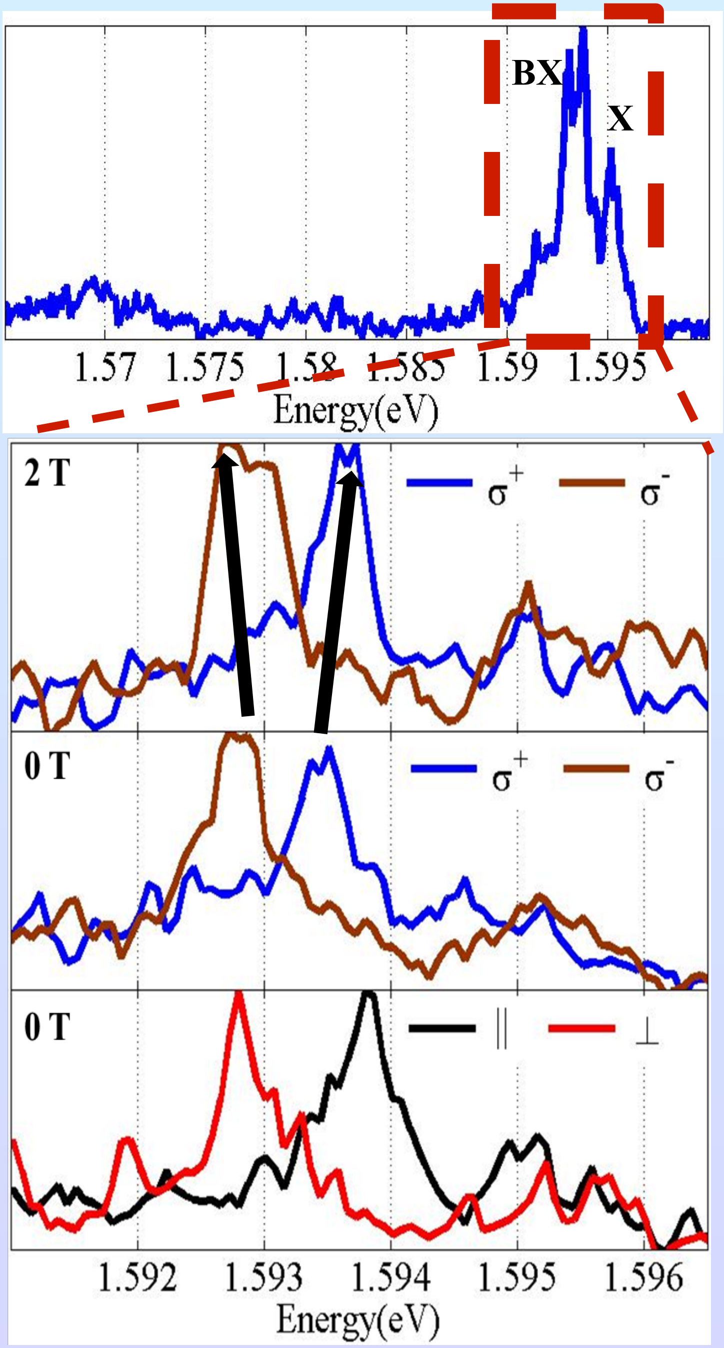
BX
X
1.57
1.575
1.58
1.585
1.59
1.595
Energy(eV)
2 T
σ^+
σ^-
0 T
σ^+
σ^-
0 T
∥
⊥
1.592
1.593
1.594
1.595
1.596
Energy(eV)

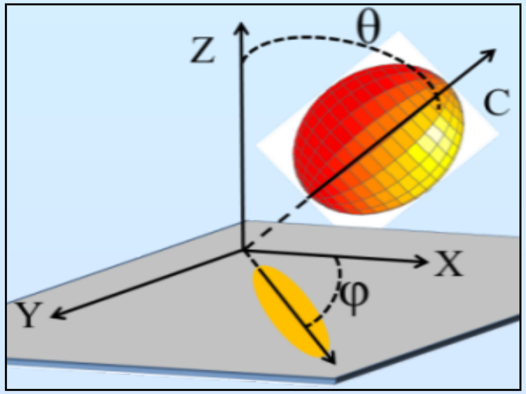
Z
θ
C
X
Y
φ

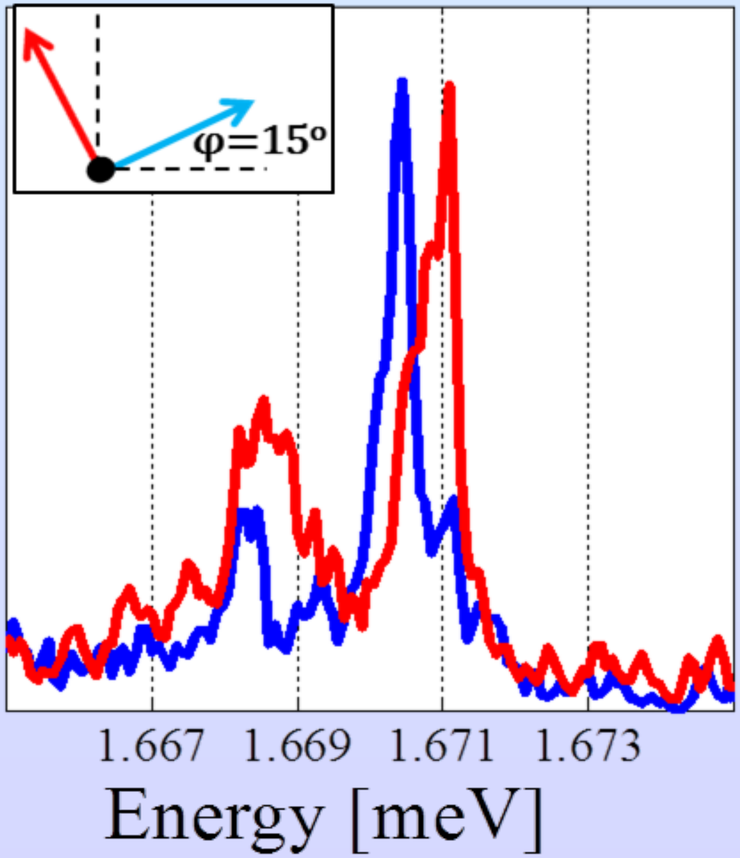
φ=15°
1.667
1.669
1.671
1.673
Energy [meV]

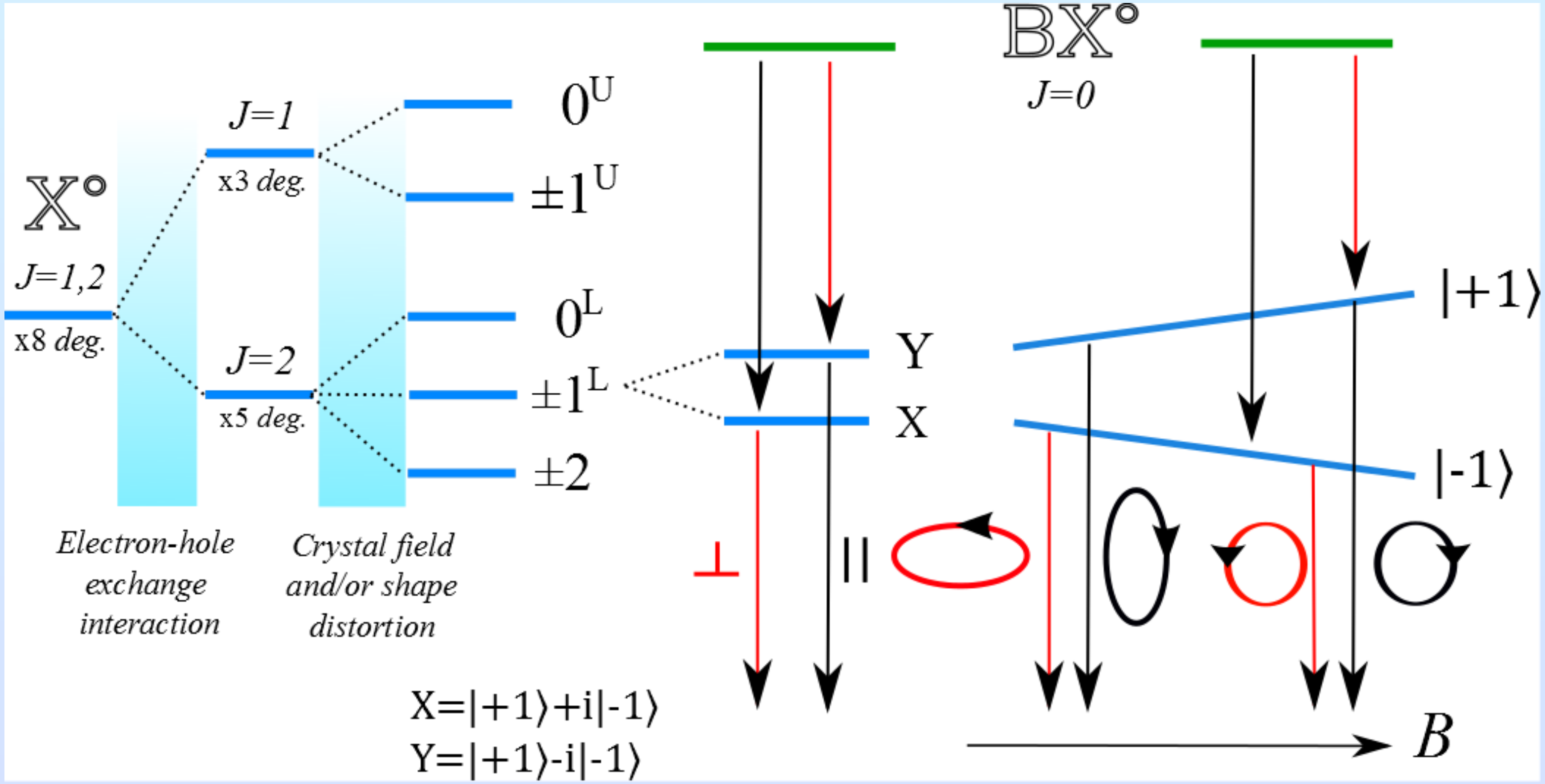

$$\Delta E_{H-V}(B) = \Delta_{exc} + \Delta_{XY}(B)$$

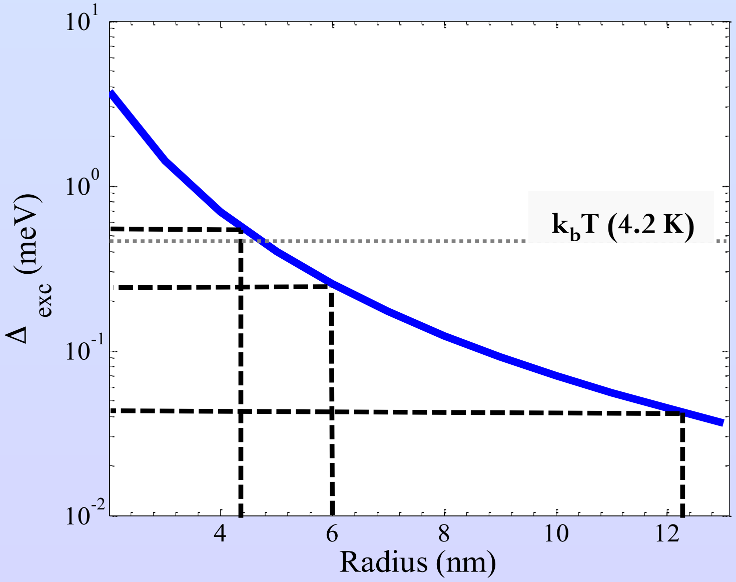

Cross Polarization Emission (B=0T)

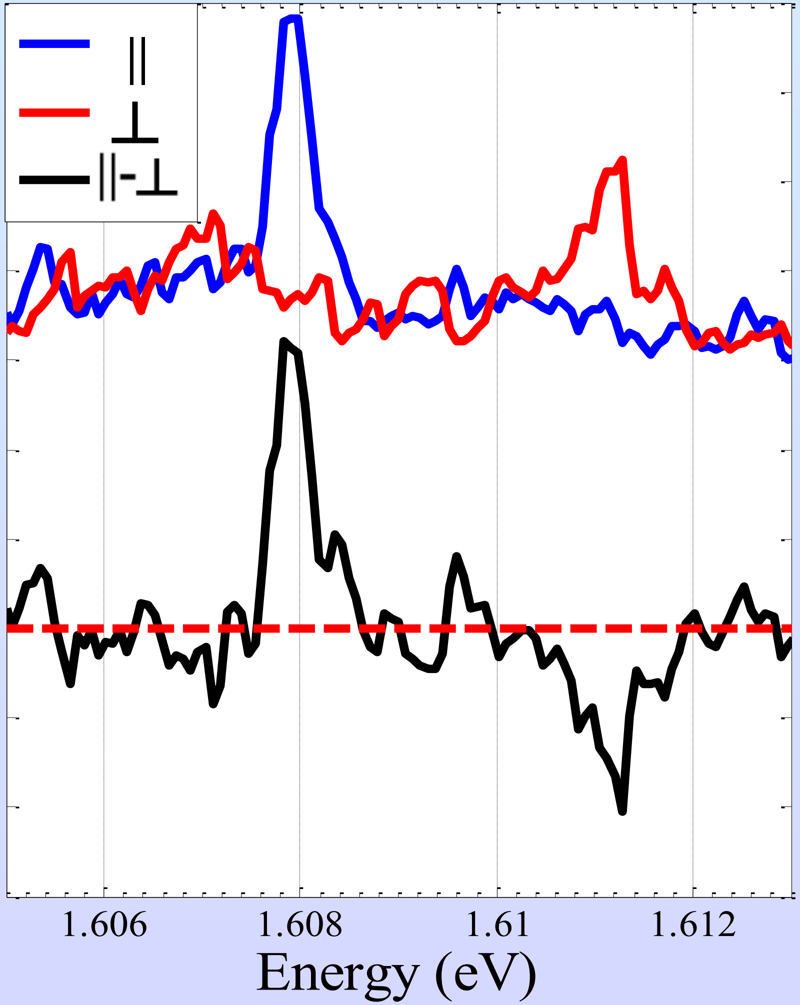

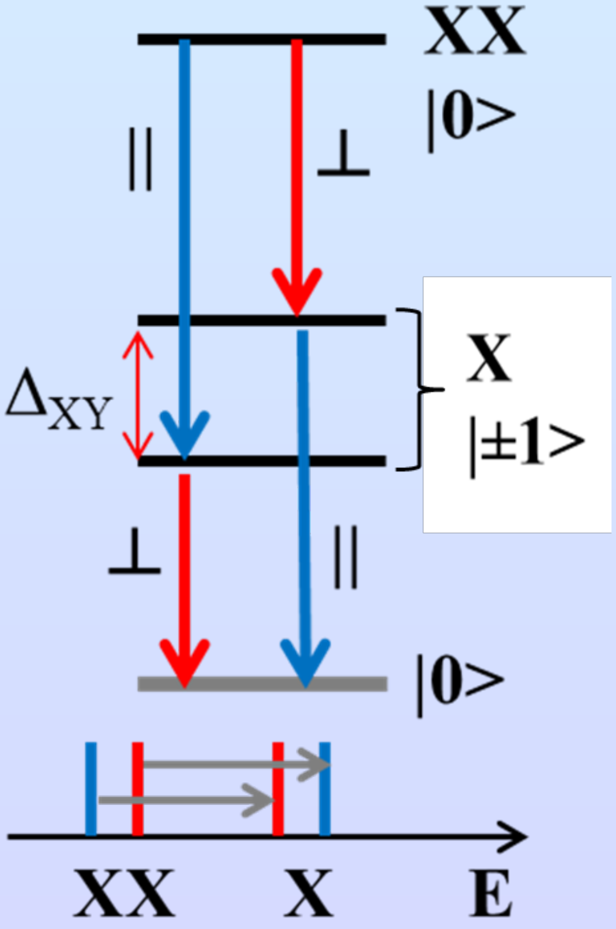

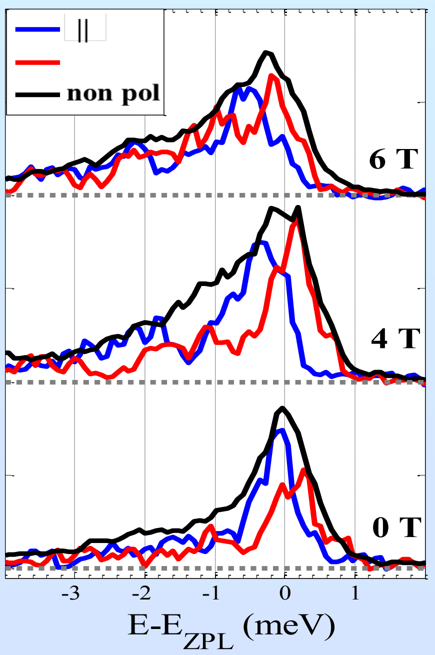

$$E_{HE/LE}(B) = E_{HE/LE}(0) \pm \frac{1}{2} g_X \mu_B B + \gamma_2 B^2$$

$$g_X \propto E_{HE}(B) - E_{LE}(B)$$

$$\gamma_2 \propto \left(E_{HE}(B) + E_{LE}(B)\right)^2$$

$$\gamma_2 = e^2 \left\langle r_X^2 \right\rangle / 8\mu$$

$$D_X = 2\left\langle r_X^2 \right\rangle^{1/2}$$

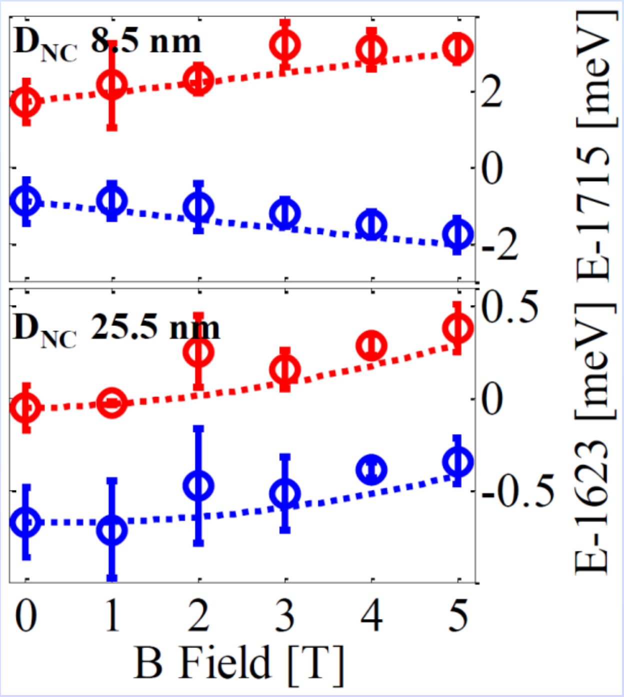

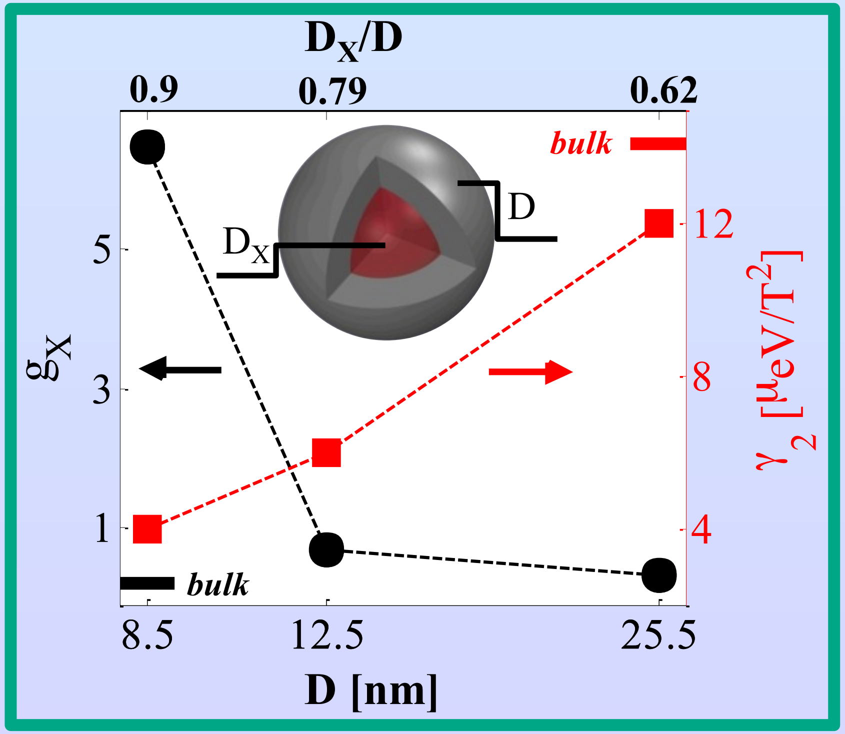

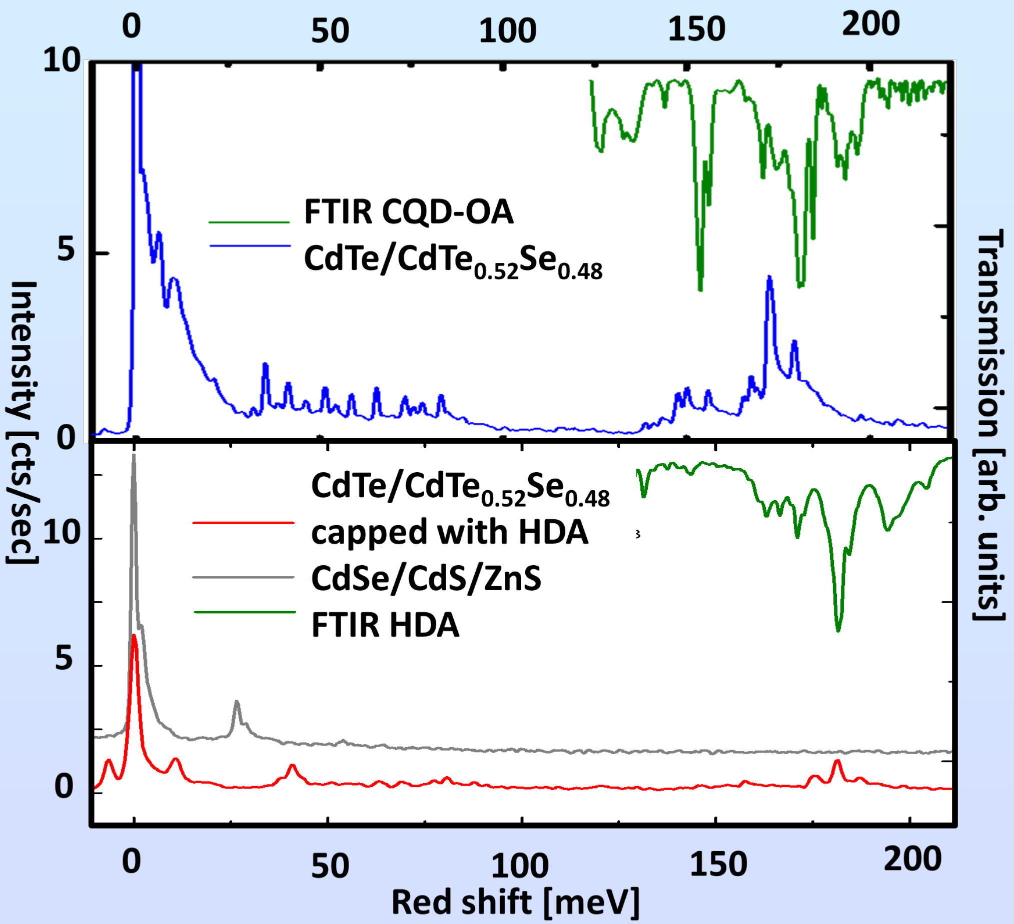
0
50
100
150
200
10
5
0
FIRT CQD-OA
CdTe/CdTe$_{0.52}$Se$_{0.48}$
CdTe/CdTe$_{0.52}$Se$_{0.48}$
capped with HDA
CdSe/CdS/ZnS
FTIR HDA
10
5
0
Intensity [cts/sec]
Transmission [arb. units]
0
50
100
150
200
Red shift [meV]

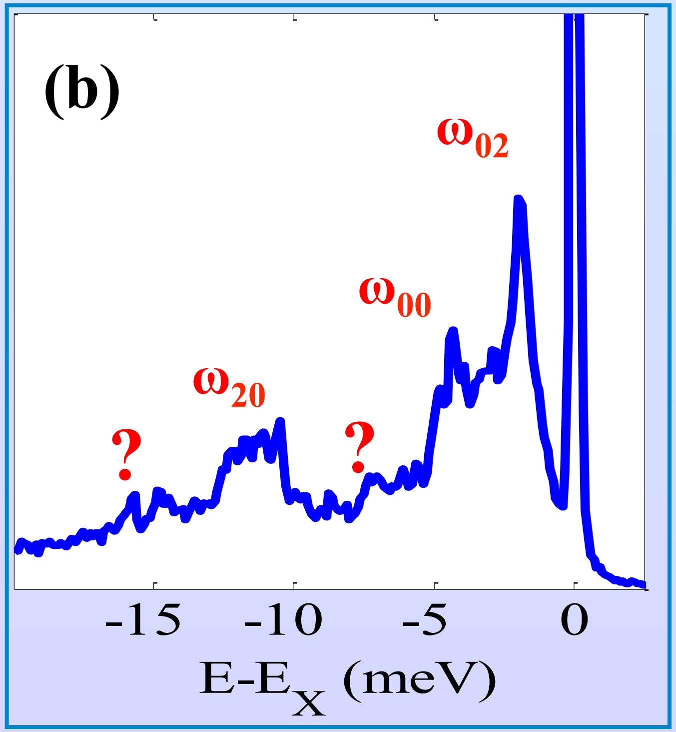
(b)
ω_{02}
ω_{00}
ω_{20}
?
?
-15
-10
-5
0
E-E$_X$ (meV)

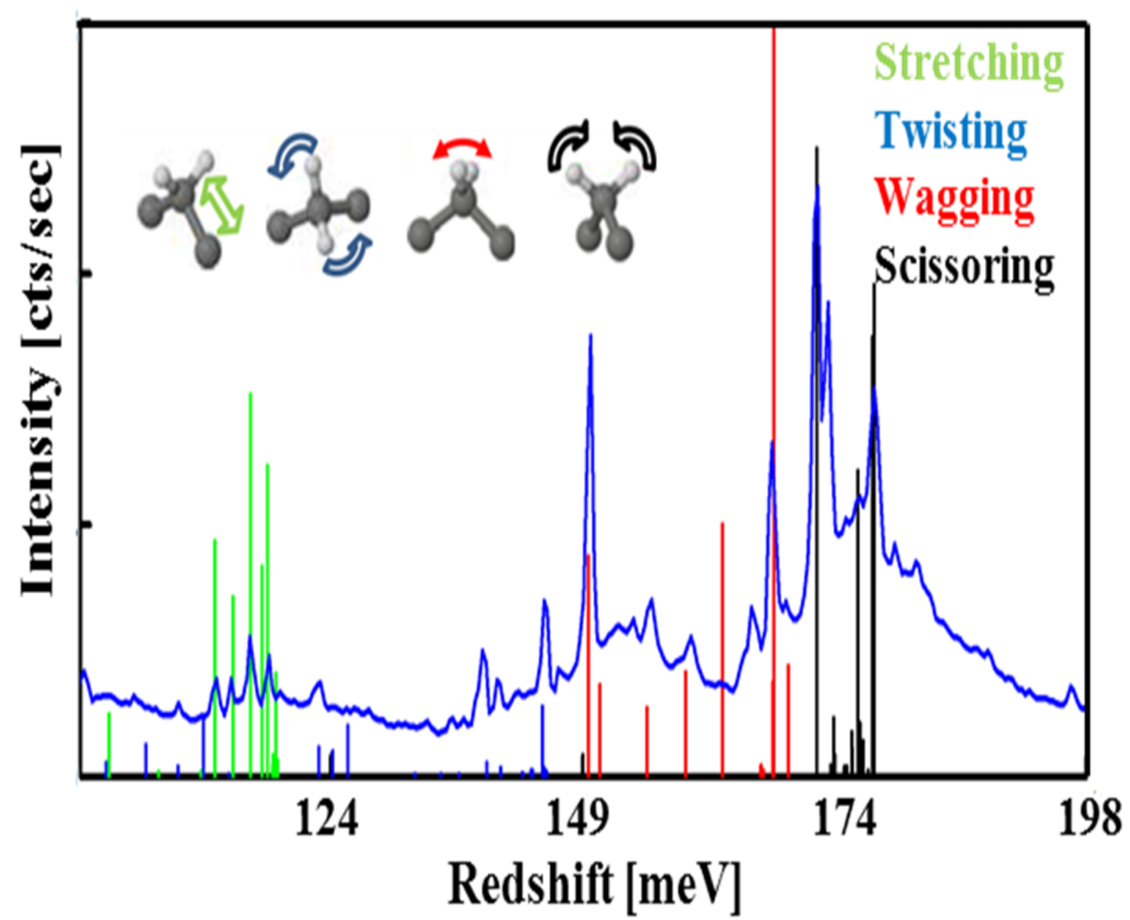
Stretching
Twisting
Wagging
Scissoring
Intensity [cts/sec]
124
149
174
198
Redshift [meV]

Influence of ligands on the transport properties

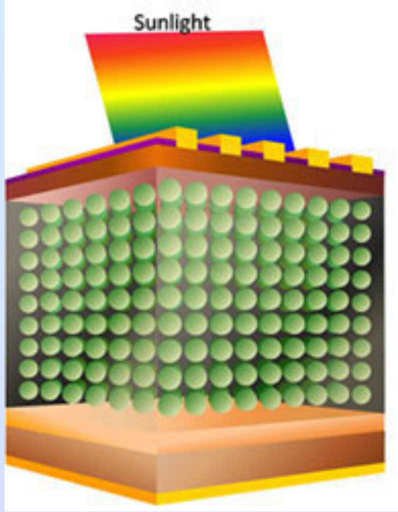

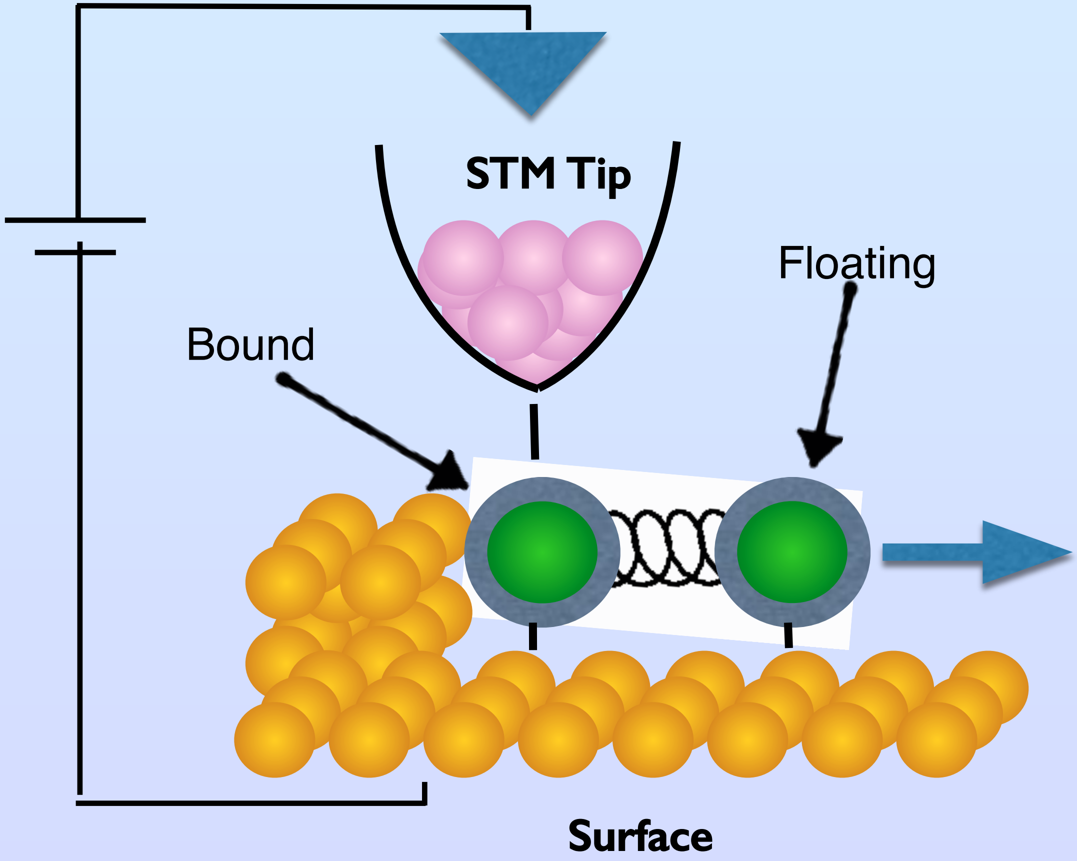

STM Tip-DQD-Surface with Mechanical Coupling

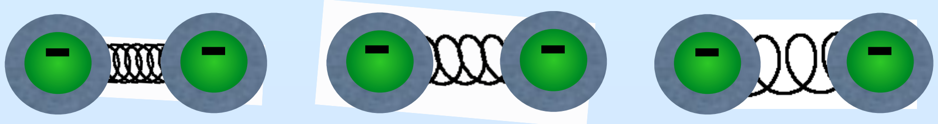

$$V(q) = D\left(e^{-2\alpha(q-q_0)} - 2e^{-\alpha(q-q_0)} + 1\right)$$

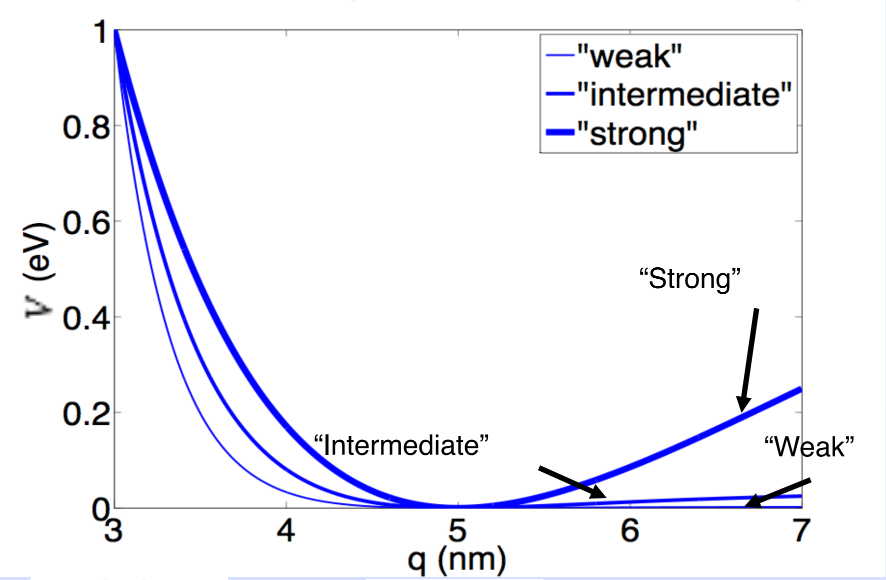

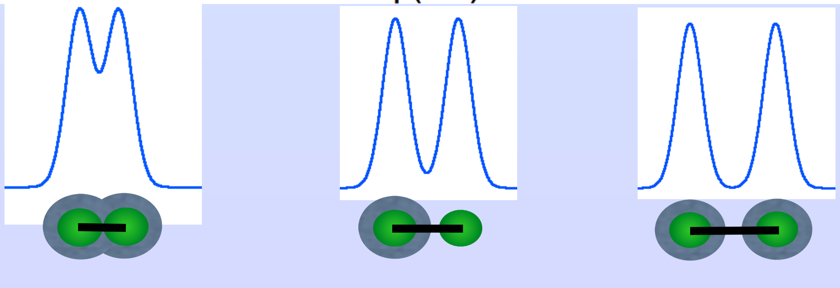

1st Measurement

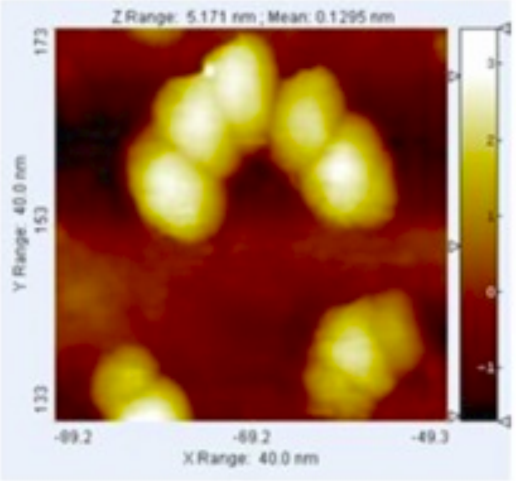

2nd Measurement

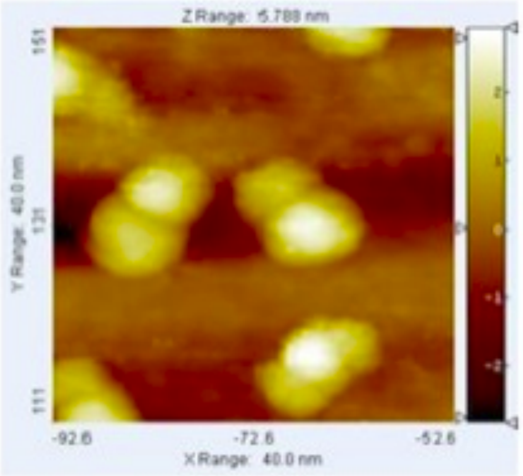

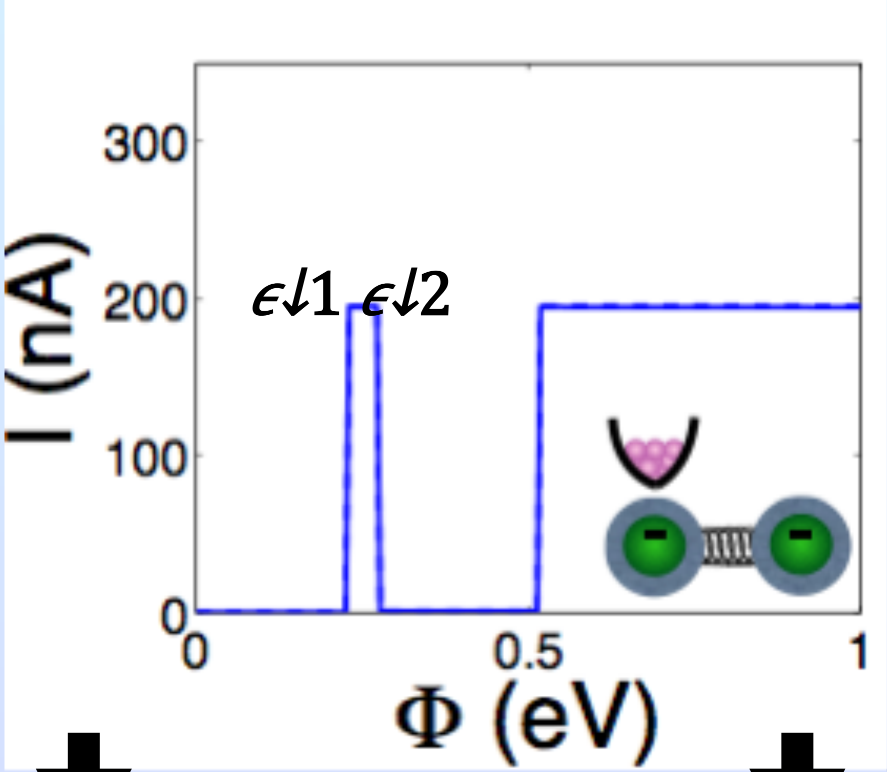

Transition Rates

T

DQD

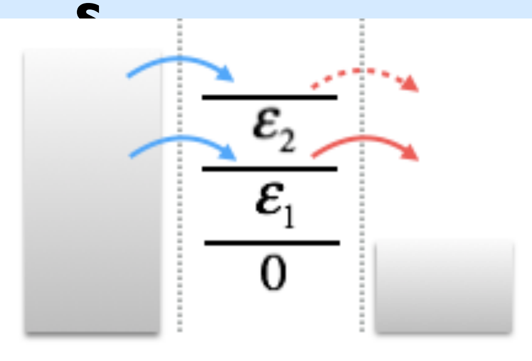

ϵ↓1

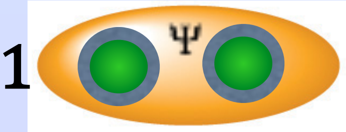

ϵ↓2

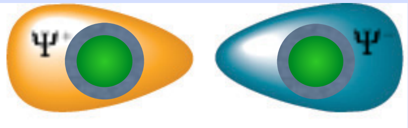

The NDR reveals the molecule-like nature of the DQD due to destructive interference in the coherent coupling to the shared surface.

Summary

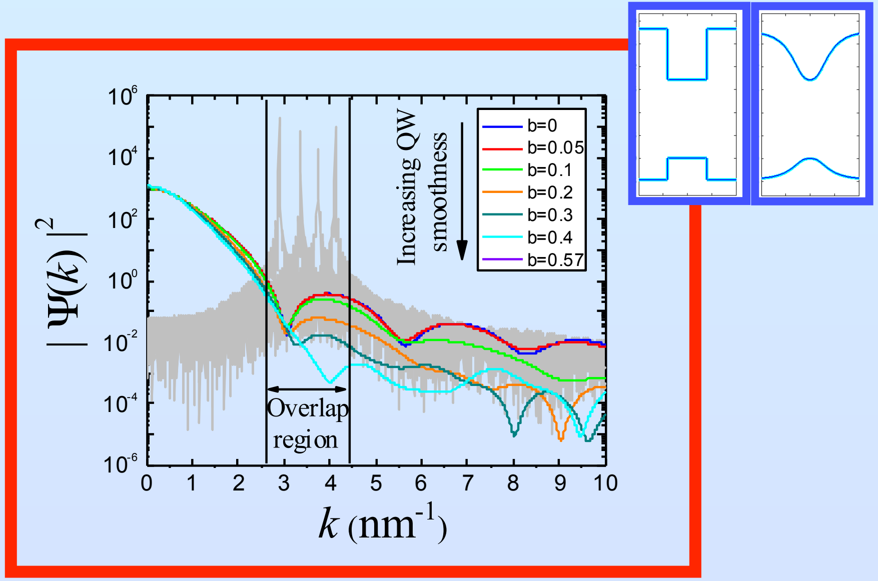

$|\Psi(k)|^2$
10^6
10^4
10^2
10^0
10^{-2}
10^{-4}
10^{-6}
0 1 2 3 4 5 6 7 8 9 10
k (nm^{-1})
Overlap region
Increasing QW smoothness
b=0
b=0.05
b=0.1
b=0.2
b=0.3
b=0.4
b=0.57

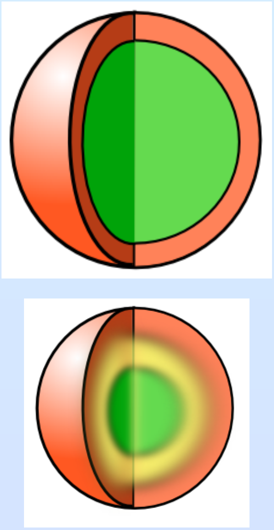

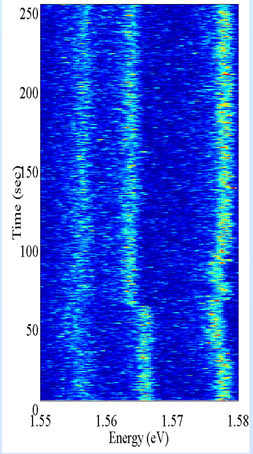

250
200
150
100
50
0
Time (sec)
1.55
1.56
1.57
1.58
Energy (eV)

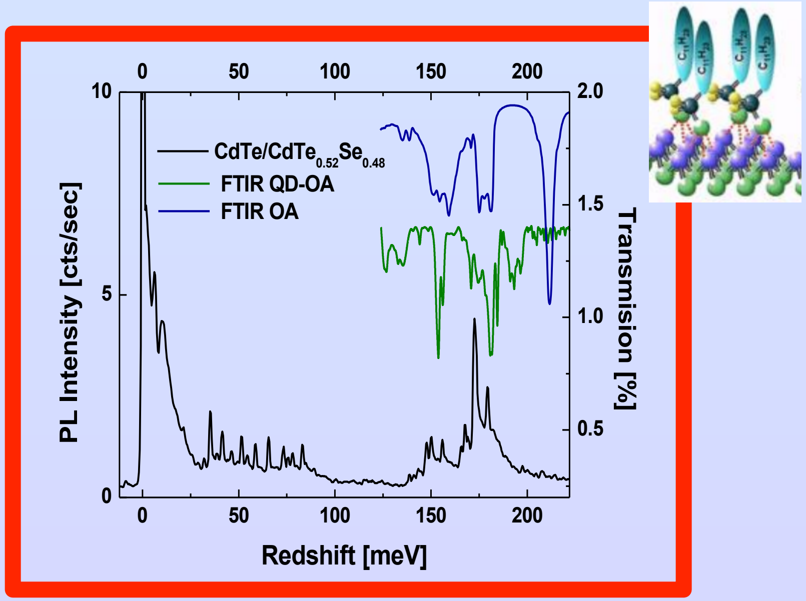

PL Intensity [cts/sec]
10
5
0
0 50 100 150 200
Redshift [meV]
Transmision [%]
2.0
1.5
1.0
0.5
CdTe/CdTe$_{0.52}$Se$_{0.48}$
FTIR QD-OA
FTIR OA
$C_{17}H_{33}$

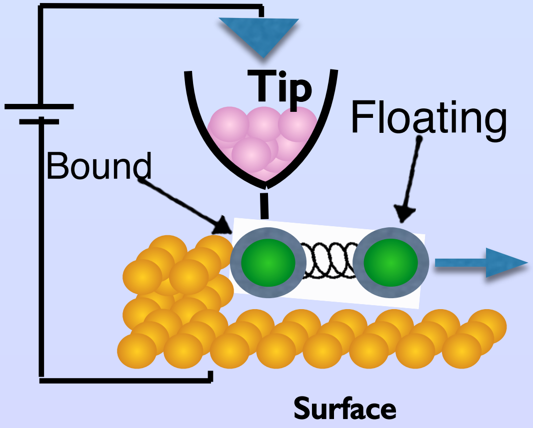

Tip
Floating
Bound
Surface

Acknowledgement: > 30 graduate students, 10 postdocs
(Most recent: G. Maikov, R. Capek, D. Yanover, A. Brusilovski, A. Sachshuik J. Tilchin, Eli Waldon, Maya Isakov, Gary Zaiats, Roni Pozner, Roman Vaxenburg, Nathan Grunbach)

Funding: European FP7 NMP projects (x2), ISF, MOS, MOT, MOD, BSF, GIF, DIP, Bikura, ITN (Horizon2020)

Open positions: postdoctoral fellows and PhD students
ssefrat@technion.ac.il

Negative Differential Resistance

Negative Resistance:

Increase in voltage results in a decrease in the current

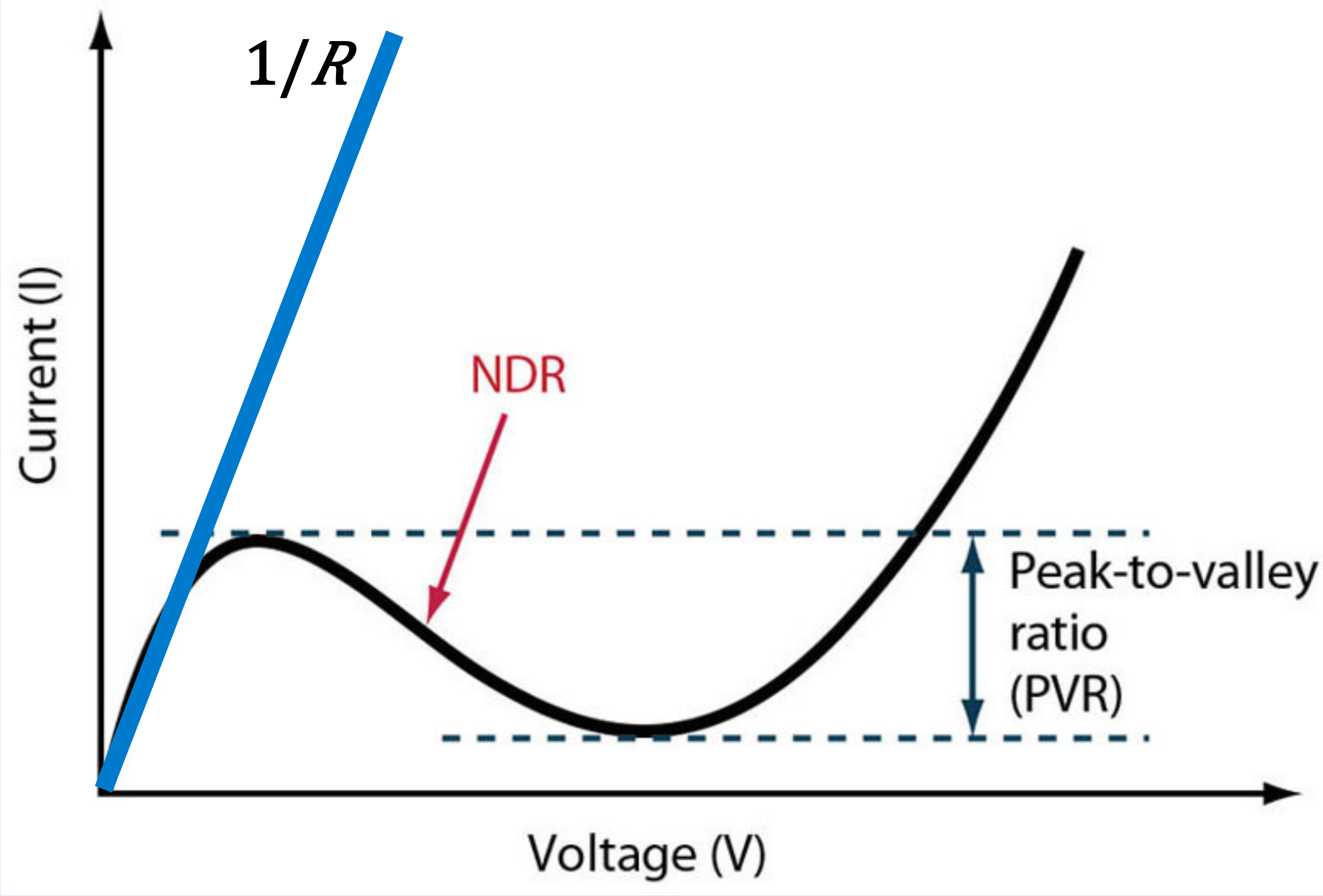

Interesting synthesis issues: Shell growth via post deposition or cation exchange

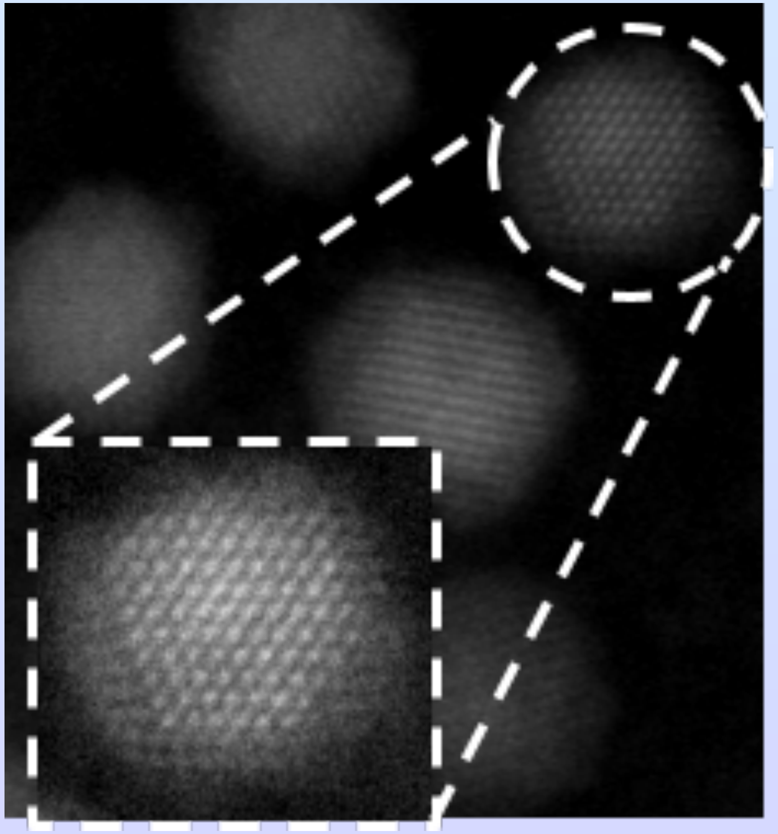

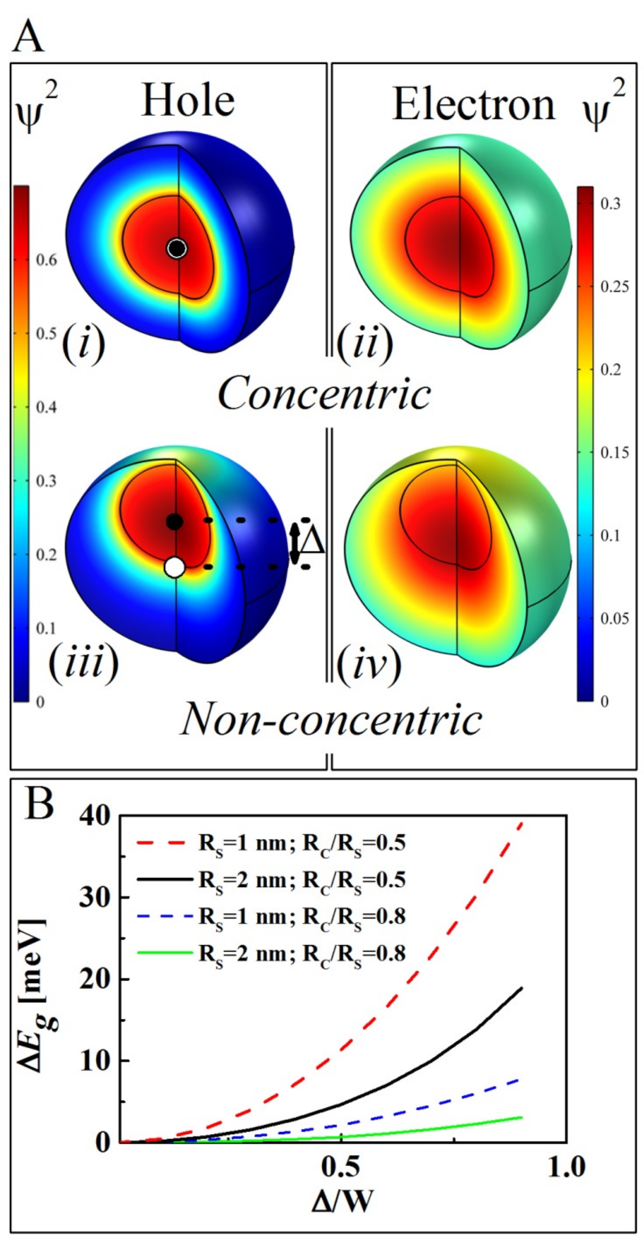

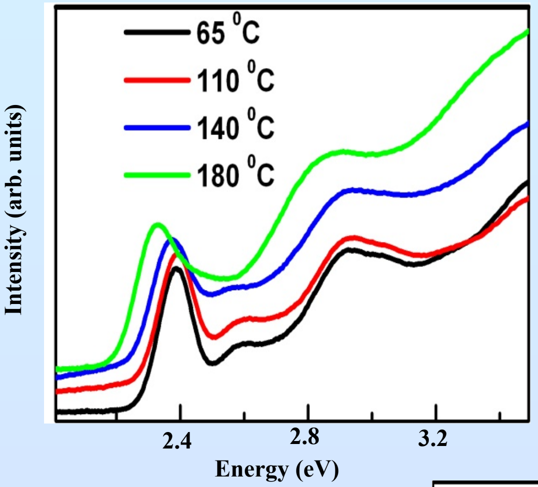
65 ^{0}C
110 ^{0}C
140 ^{0}C
180 ^{0}C
Intensity (arb. units)
2.4
2.8
3.2
Energy (eV)

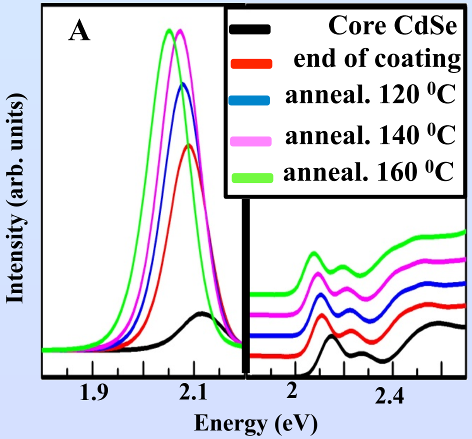
A
Core CdSe
end of coating
anneal. 120 ^{0}C
anneal. 140 ^{0}C
anneal. 160 ^{0}C
Intensity (arb. units)
1.9
2.1
2
2.4
Energy (eV)

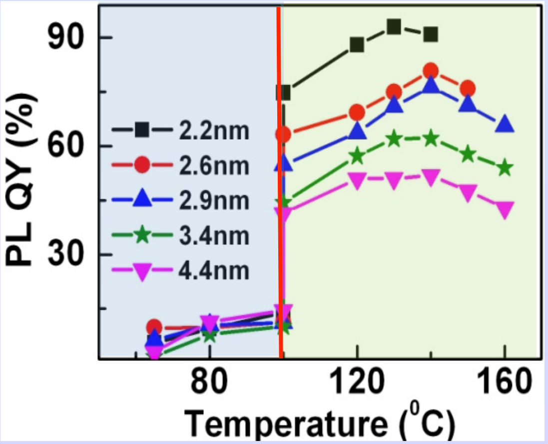
90
60
30
PL QY (%)
2.2nm
2.6nm
2.9nm
3.4nm
4.4nm
80
120
160
Temperature (^{0}C)

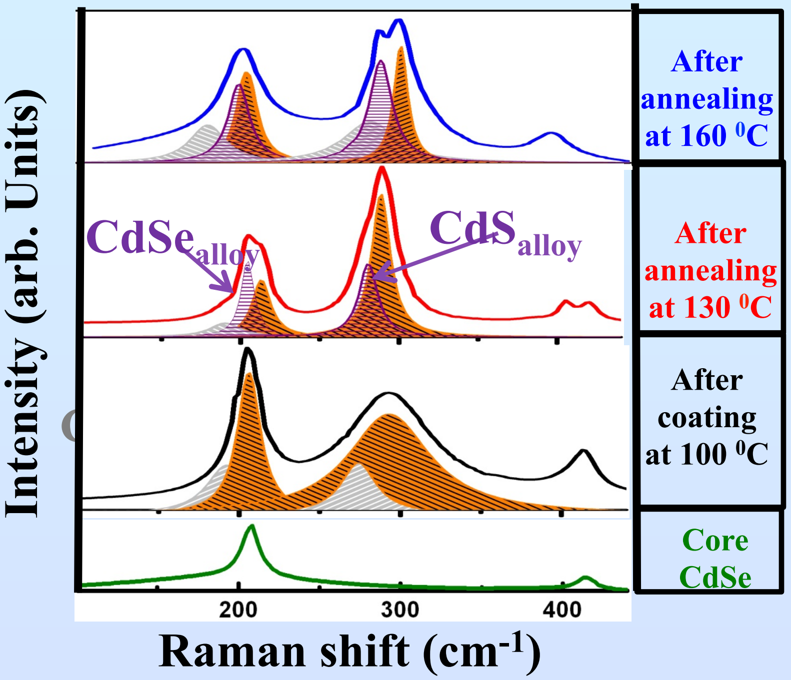
After annealing at 160 ^{0}C
After annealing at 130 ^{0}C
After coating at 100 ^{0}C
Core CdSe
CdSe$_{alloy}$
CdS$_{alloy}$
Intensity (arb. Units)
200
300
400
Raman shift (cm^{-1})

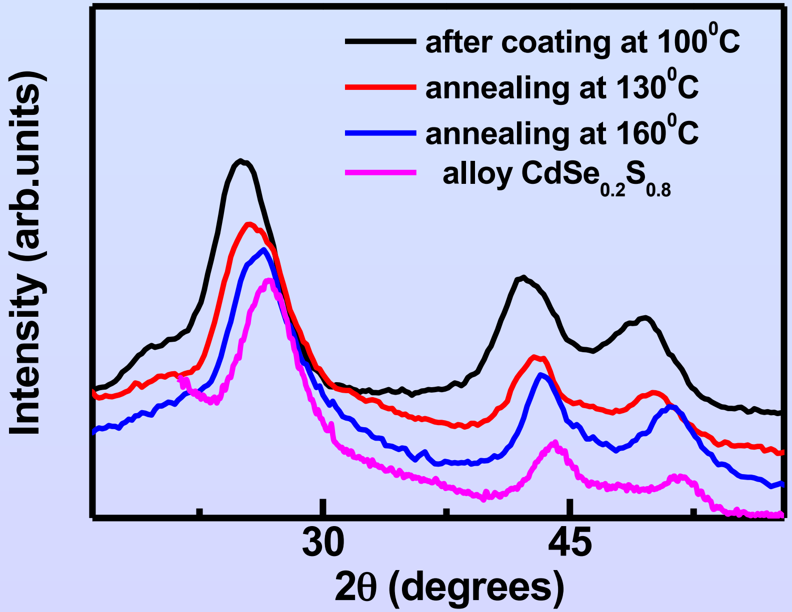
after coating at 100^{0}C
annealing at 130^{0}C
annealing at 160^{0}C
alloy CdSe$_{0.2}$S$_{0.8}$
Intensity (arb.units)
30
45
2θ (degrees)

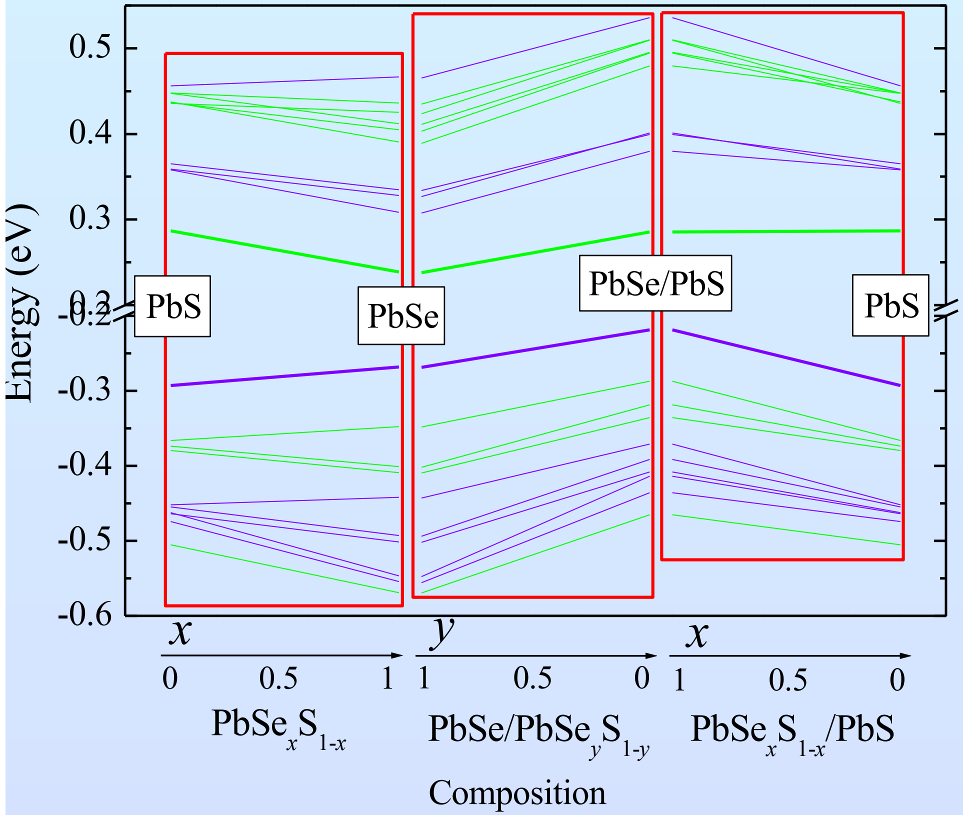
Energy (eV)
0.5
0.4
0.3
0.2
-0.2
-0.3
-0.4
-0.5
-0.6
PbS
PbSe
PbSe/PbS
PbS
x
0
0.5
1
y
1
0.5
0
x
1
0.5
0
$PbSe_xS_{1-x}$
$PbSe/PbSe_yS_{1-y}$
$PbSe_xS_{1-x}/PbS$
Composition

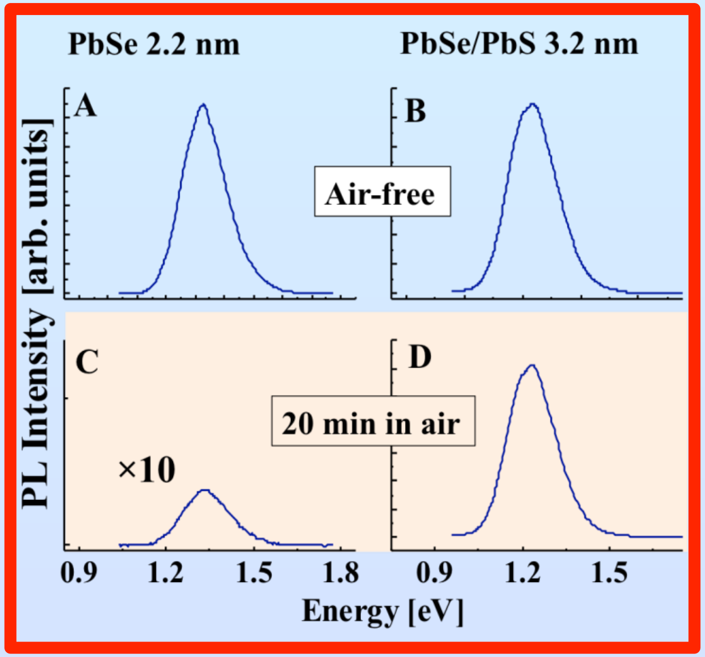
PbSe 2.2 nm
PbSe/PbS 3.2 nm
A
B
Air-free
C
D
20 min in air
×10
PL Intensity [arb. units]
0.9
1.2
1.5
1.8
0.9
1.2
1.5
Energy [eV]

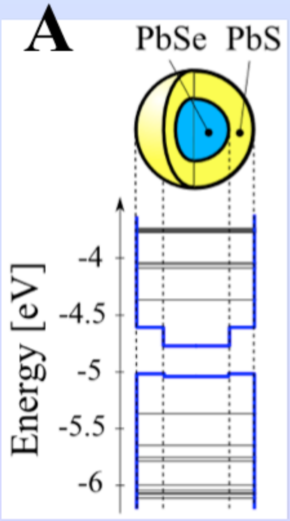
A
PbSe
PbS
Energy [eV]
-4
-4.5
-5
-5.5
-6

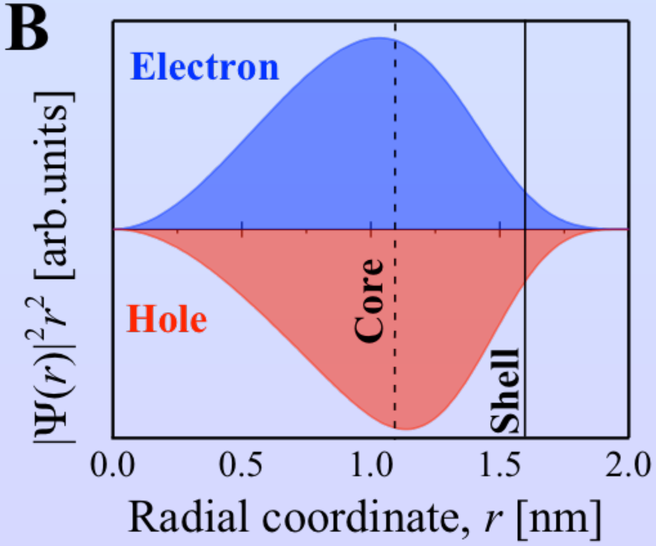
B
Electron
Hole
Core
Shell
$|\Psi(r)|^2r^2$ [arb.units]
0.0
0.5
1.0
1.5
2.0
Radial coordinate, r [nm]

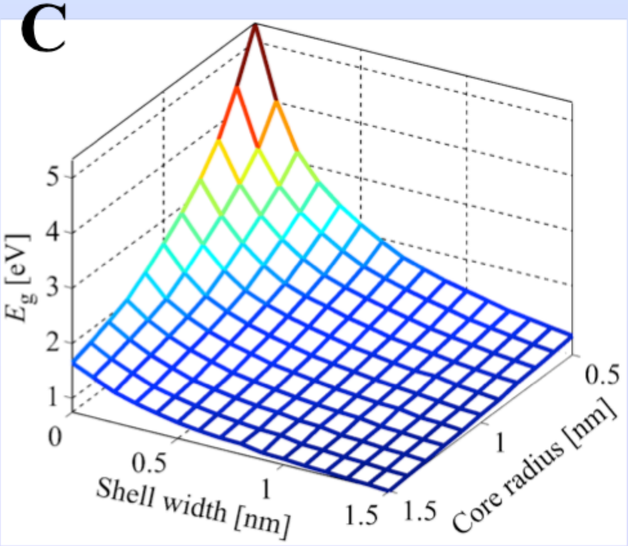
C
E_g [eV]
0
1
2
3
4
5
0.5
1
1.5
Shell width [nm]
0.5
1
1.5
Core radius [nm]

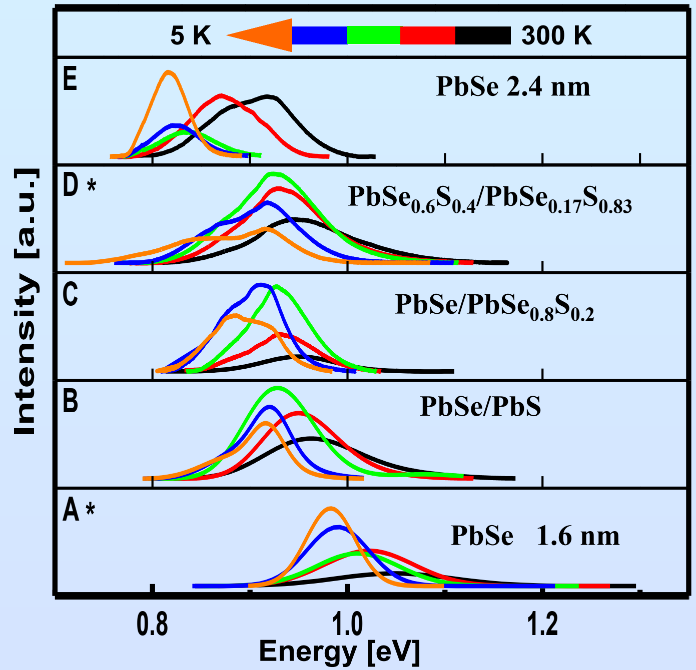
5 K
300 K
E
PbSe 2.4 nm
D *
$PbSe_{0.6}S_{0.4}/PbSe_{0.17}S_{0.83}$
C
$PbSe/PbSe_{0.8}S_{0.2}$
B
PbSe/PbS
A *
PbSe 1.6 nm
Intensity [a.u.]
0.8
1.0
1.2
Energy [eV]

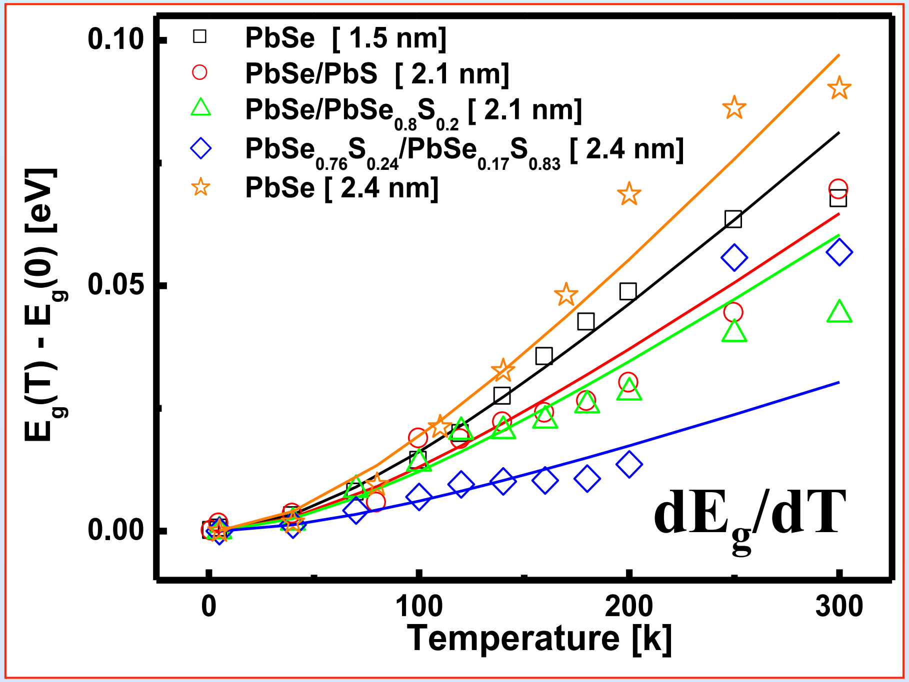
0.10
0.05
0.00
$E_g(T) - E_g(0)$ [eV]
PbSe [1.5 nm]
PbSe/PbS [2.1 nm]
$PbSe/PbSe_{0.8}S_{0.2}$ [2.1 nm]
$PbSe_{0.76}S_{0.24}/PbSe_{0.17}S_{0.83}$ [2.4 nm]
PbSe [2.4 nm]
dE_g/dT
0
100
200
300
Temperature [k]

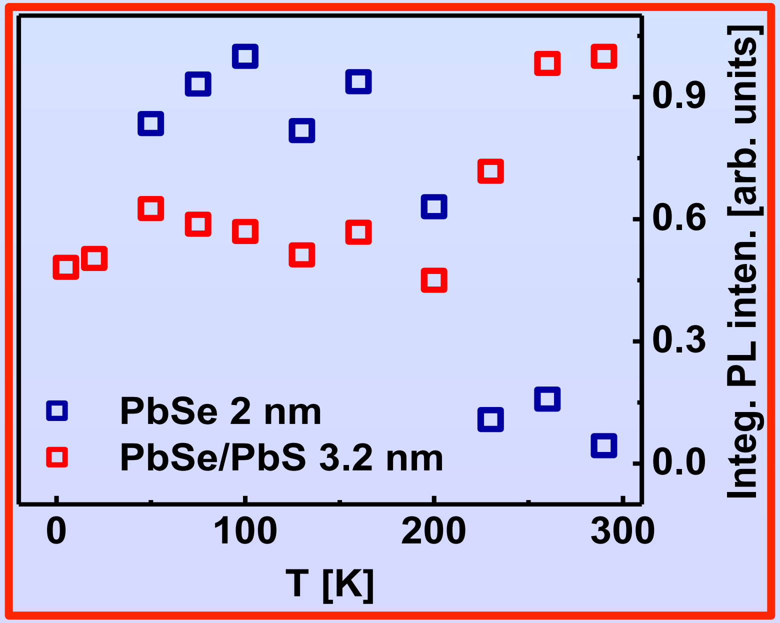
PbSe 2 nm
PbSe/PbS 3.2 nm
0.9
0.6
0.3
0.0
Integ. PL inten. [arb. units]
0
100
200
300
T [K]

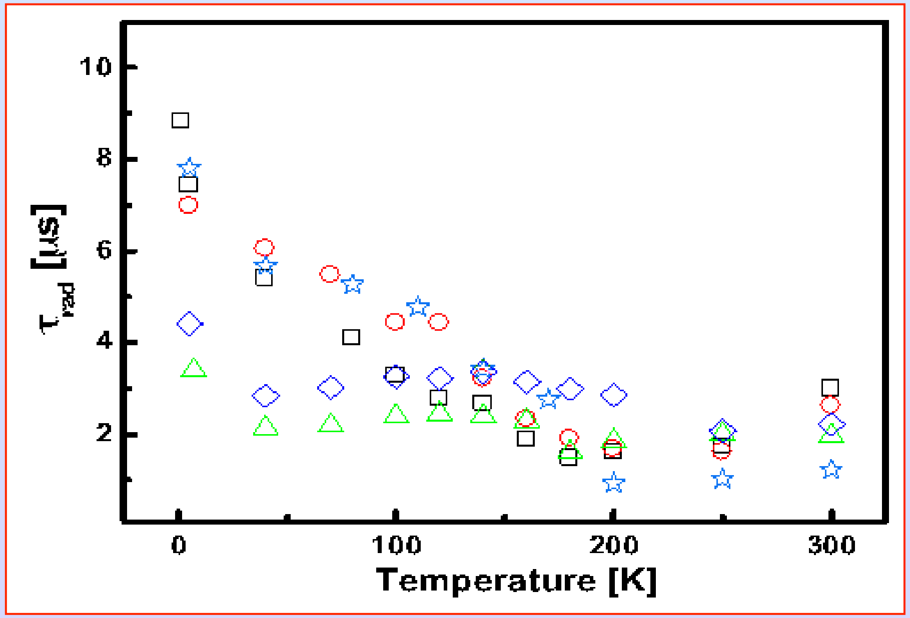
10
8
6
4
2
τ_{rad} [µs]
0
100
200
300
Temperature [K]